THESIS

HYDROLOGIC IMPACTS OF LINED GRAVEL PITS, COLORADO FRONT RANGE

Submitted by

Gavin Rach

Department of Geosciences

In partial fulfillment of the requirements

For the Degree of Master of Science

Colorado State University

Fort Collins, Colorado

Fall 2018

Master's Committee

Advisor: Michael Ronayne

Ryan Bailey
William Sanford

ABSTRACT

HYDROLOGIC IMPACTS OF LINED GRAVEL PITS, COLORADO FRONT RANGE

Sand and gravel quarries are a major source of natural aggregate. Gravel pits often excavate below the water table and therefore can influence alluvial aquifer groundwater flow directions and groundwater-surface water interaction. By regulation in the state of Colorado, low-permeability liners are installed after extraction to minimize water seepage into the pit. The liner impedes flow and disturbs the local water table, creating mounding on the upgradient side and shadow drawdown on the downgradient side. To better understand the magnitude and extent of these effects, numerical groundwater modeling was conducted for a study area along the Saint Vrain Creek alluvial aquifer in Colorado that contains an active gravel pit. The numerical model was based on a revised conceptual model, including a reinterpretation of the bedrock surface, and was calibrated using measured groundwater levels and estimated groundwater-surface water exchange rates constrained by streamflow gaging data. Two transient modeling scenarios were developed: a base case pre-mining scenario and a post-mining lined-pit scenario. The hydrologic effects of the pit liner were quantified through a detailed comparison of the scenarios.

Model results indicate that the liner has a significant effect on water-table elevation in the vicinity of the pit during the non-irrigation season (October-March). In March, upgradient mounding produced by the liner exceeds 0.5 m at an approximate distance of 100 m, whereas the drawdown exceeds 0.3 m at this distance on the downgradient side of the pit. The magnitude of these liner-induced changes is less than other seasonal variability in hydraulic head, particularly the variability associated with irrigated agriculture (seasonally active irrigation ditches). During

the irrigation season, simulated hydraulic heads are similar in both model scenarios, demonstrating that irrigation ditches are a major control on groundwater flow. Despite significant water table elevation change in parts of the year, groundwater discharge to the stream increased by 0.11% of the total streamflow at its maximum, demonstrating this particular pit liner has a negligible effect on the Saint Vrain Creek.

ACKNOWLEDGEMENTS

I would like to express my deepest appreciation and gratitude for my advisor, Dr. Michael Ronayne, for his unrelenting patience and supporting me through my academic journey. He has been a great resource, role model, and teacher—helping prepare me for an exciting career in the environmental sector.

I would also like to give special thanks to the Varra Companies, Inc. for sponsoring this research and providing an exciting opportunity to work on a relevant and challenging topic for my dissertation.

Graduate school can be an arduous path for nearly anyone. Because of that I would like to thank all the great friends (geologists in training) I met in the CSU Department of Geosciences for the support network we provided each other. We spent many nights bouncing research ideas and problems off of each other and many others just in good company. They were truly invaluable through my academic journey.

Finally, I would like to thank my family for supporting me through my decisions to pursue this career path. Even though they were far away, it was nice to know I had support from my hometown as well as at school.

TABLE OF CONTENTS

LIST OF TABLES

LIST OF FIGURES

Figure 16: Simulated water table change at the end of four months of the year. Negative values indicate a predicted water table increase (mounding), whereas positive values indicate a decrease in the water table elevation (drawdown).

CHAPTER 1: INTRODUCTION

Sand and gravel quarries are a major source of natural aggregate important for the concrete industry, infrastructure, and various other uses. In 2016 approximately 6,300 sand and gravel mining operations produced 1.01 billion tons valued at $8.9 billion across 50 states, making it the second most important source for aggregate in the U.S (Ober, 2017). With demand for aggregate growing nearly every year, new sources of sand and gravel are highly valued. High quality sand and gravel deposits are typically found in river valleys and floodplains as seen in the South Platte River and its tributaries along the Colorado Front Range (Schwochow, Shroba, & Wicklein, 1974; Lindsey, Langer, Cummings & Shary 1998). These geological environments are a prime target for sand and gravel quarries but are also an important source for shallow groundwater in the form of alluvial aquifers. There is often a fine balance between acquiring this valuable resource and minimizing impact to Colorado's relatively scarce water resources.

Economical gravel deposits are often located in the saturated zone, especially in areas with shallow water tables. Open pit mining below the water table can influence local hydrology both during excavation and post-reclamation. In an effort to minimize the evaporation of groundwater in Colorado's semi-arid climate, the Colorado Legislature passed Senate Bill 120 in 1989 requiring water replacement plans for any gravel pit which exposes groundwater. To prevent this from occurring continuously, excavated gravel pits are lined with a low permeability material, also known as a slurry wall, to mitigate groundwater seepage into the mine and reduce groundwater exposure to evaporation. Pit liners must be designed in accordance with the Colorado state engineer's guidelines (Colorado Division of Water Resources [CDWR], 1999) to achieve significantly low levels of groundwater seepage into the pit. Some post-mining

reclamation plans allow for open pits to be converted to artificial lakes for recreation. However, the liner requirement is designed to limit the amount of surface water features hydraulically connected to adjacent alluvial aquifers.

While slurry walls help to prevent groundwater exposure to Colorado's dry climate, these low-permeability features also have the potential to impact the water table elevation and groundwater flow directions in alluvial aquifers. Lined pits may act as a laterally and vertically extensive barrier to groundwater flow, forcing flow around the pit—especially because a large number of these pits are excavated down to bedrock. Installation of a low-permeability liner can result in mounding on the upgradient side and drawdown, also known as a "shadow drawdown" effect, on the downgradient side of the pit. A previous study by the U.S. Geological Survey documented these effects through use of analytical and numerical solutions in hypothetical aquifer settings (Arnold, Langer, & Paschke, 2003). Their results illustrated that a liner can produce mounding and drawdown that was not previously present. The magnitude of these changes is dependent on a variety of site-specific factors.

Sand and gravel quarries do not inherently cause major water table fluctuations. A study in Minnesota monitored two active and unlined pits and concluded there was little to indistinguishable influence on the local water table (Green, Pavlish, Merritt, & Leete 2005). Fluctuations in the water table were attributed to precipitation events. These sites did not undergo dewatering and were instead mined by way of dredging. Lined pits undergo mine dewatering before and during excavation as the slurry wall is emplaced to prevent seepage into the pit. There are limited studies that explore the impacts of a lined pit distinguishing the long-term effects of the liner over the short-term effects of dewatering recovery.

A major challenge lies in quantifying the hydrological effects of lined pits. Changes in groundwater flow patterns directly attributable to these features can be difficult to measure. Significant amounts of time pass between excavation, mine completion and liner installation, before the water table can return to a state similar to pre-excavation. Aside from time, another challenge lies in distinguishing these effects from other human influences, mine dewatering, seasonal fluctuations, and interannual variability in water table elevations, all dependent upon the area.

The goal of this paper is to better understand the hydrological effects, including water-table changes and changes in groundwater-surface water exchange, associated with liner installation in gravel pits that have fully excavated to bedrock. These effects are investigated for a study area along St. Vrain Creek, Colorado, that includes an existing open-pit aggregate mine. Steady-state and transient (seasonal) numerical model simulations are performed to evaluate the potential hydrological changes in the vicinity of pit liners. A numerical model using MODFLOW is used to simulate the effects of a long-term, steady-periodic groundwater flow system during a representative year with and without lined pits. The modeling analysis takes into account how seasonal factors like irrigation influence the water-table position, and how these factors compare to the effects of pit liners.

CHAPTER 2: SITE DESCRIPTION

2.1 Regional Hydrogeologic Setting

The South Platte River (including its tributaries) alluvial aquifer system encompasses most of northeastern Colorado's shallow groundwater resources. Tributary to the South Platte, the St. Vrain Creek watershed drains the foothills north of Boulder, CO, bringing sediments eroded from granitic and gneissic bedrock to the lower gradient floodplains of the Front Range (Figure 1).

The area of interest for this study lies between the Boulder Creek confluence and the mouth of St. Vrain Creek, where it joins the South Platte River (Figure 2). Natural aggregate resources are abundant and high in quality as evidenced by the sheer amount of gravel pit development in the area. This stretch of the St. Vrain alluvial valley is geologically characterized by coarse-grained sand and pebble gravel (Schwochow et al., 1974). The relatively thin alluvial deposits average 6-9 meters in thickness but can be as thick as 15 meters towards the mouth. Areas outside the alluvium are dominated by Upper Holocene fine-grained eolian deposits (Colton, 1978). The alluvial valley is underlain by the Pierre Shale, Laramie-Fox Hills sandstone (LFH), and the Laramie confining layer--all Upper Cretaceous in age (Robson, Van Slyke & Graham, 1998). Nearly all of the northwestern alluvial boundary is formed by bedrock outcroppings of both the Pierre shale and LFH sandstone (Robson, Heiny, & Arnold, 2000a, 2000b).

A remarkably similar alluvial valley can be seen in sections of the South Platte River (Figure 3). In cross section H3, the South Platte River is bounded by bedrock on one side, and high-quality aggregate deposits on the other with eolian deposits even further in the same

direction. As the valley floor rises, increasing amounts of eolian clay and silt can be found until it dominated the unconsolidated material column (Lindsey et al., 1998).

Streamflow in St. Vrain Creek is measured at two gaging stations in the region (Figure 2). Flow typically varies from as low as 250,000 m^3/d in the winter to approximately ten times as much during early summer. Water diversion from Saint Vrain Creek into the primary irrigation ditch can occur between late March to early November, but most consistently from May to September. Diversions have historically ranged from 1,000 m^3/d to nearly 200,000 m^3/d during summer months (CDWR, 2017). The primary irrigation ditch in the area returns excess water to the floodplain downstream.

The alluvial aquifer in this area is generally quite shallow and thin. Depth to the water table is less than 6 meters, and the saturated thickness ranges from a few meters in some places to 12-15 meters in others (Robson et al., 2000a; 2000b). Groundwater in the alluvial aquifer flows primarily to the northeast, following the flow direction of Saint Vrain Creek. The hydraulic gradient is between .003 and .002, lessening towards the mouth of the river. Previous regional water table maps also indicate a strong north-northwest flow direction from eolian deposits into the alluvial aquifer (Robson et al., 2000; Schneider, 1983; CDM Smith, 2013). Three pumping tests have been conducted in the alluvium within the study area; reported hydraulic conductivity values from these tests were 38.1, 220, and 85.6 m/d (AWES, 2015; Smith, Schneider, & Petri, 1964) with an average of 114.6 m/d. All tests were near the edge of the alluvium, bordering eolian deposits, at significant distances from the river.

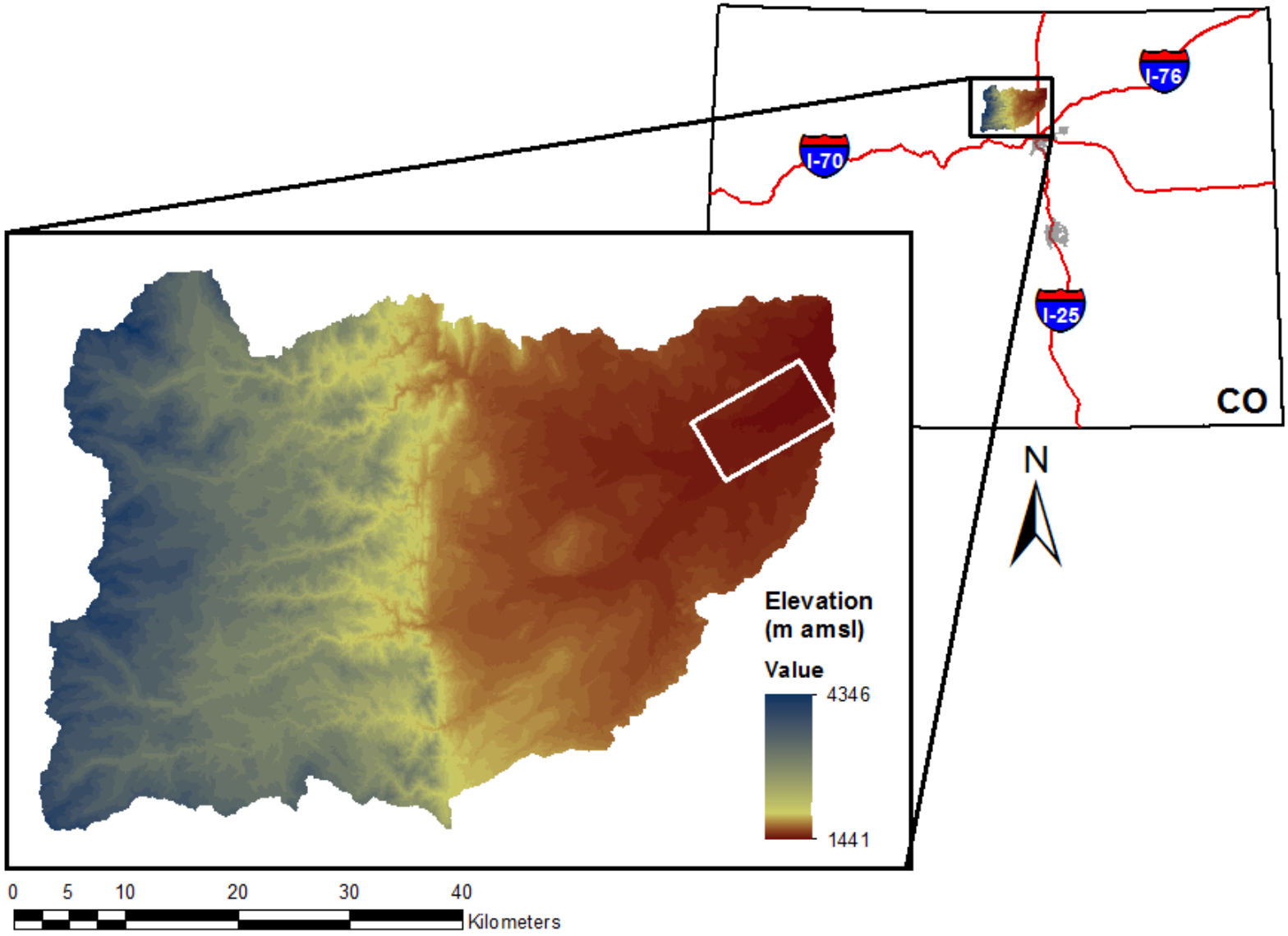

Figure 1: Location of study area in Saint Vrain Creek Watershed and the state of Colorado.

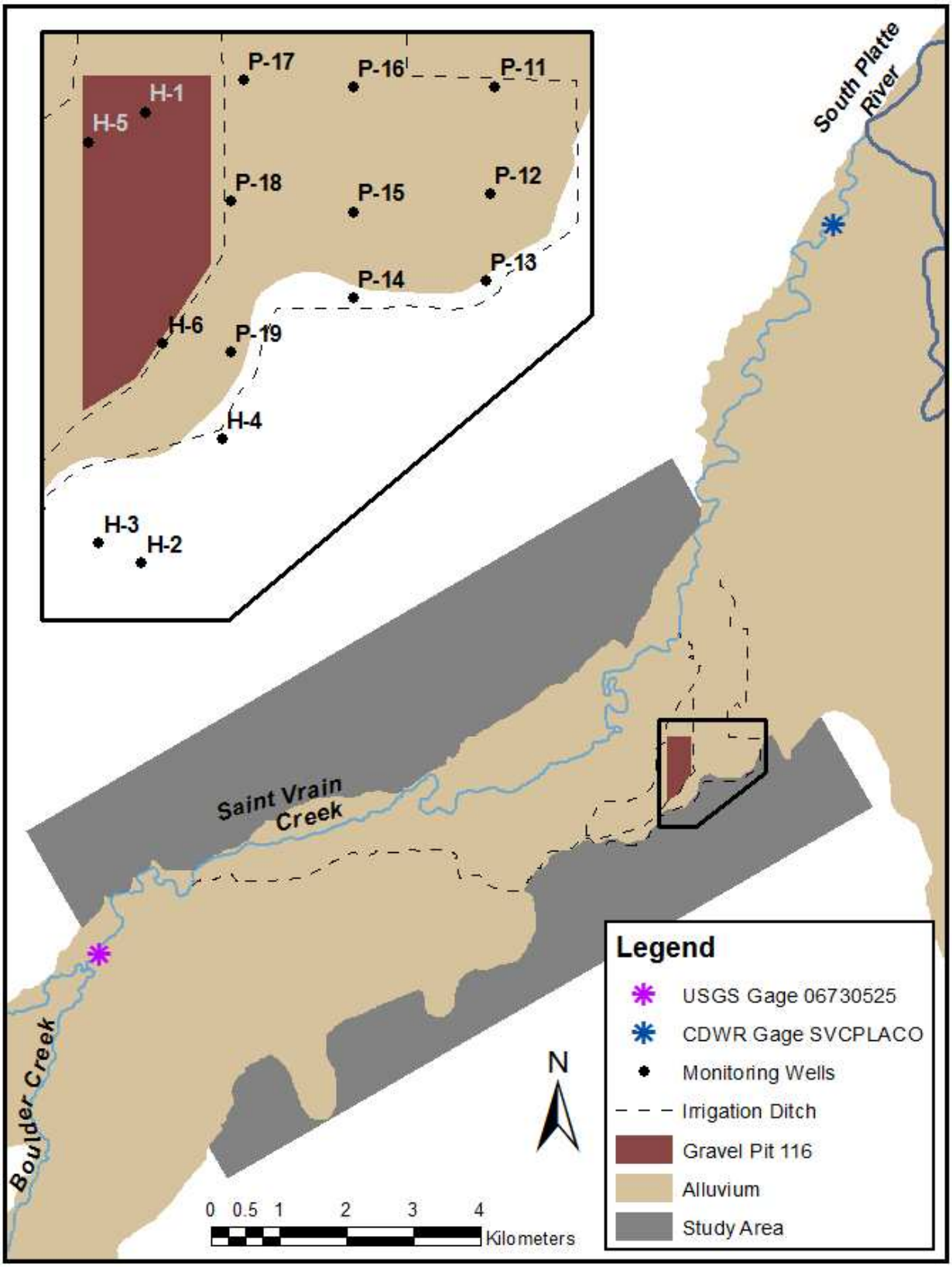

Figure 2: Map of study area showing mine location, mine site monitoring wells, and Saint Vrain stream gages.

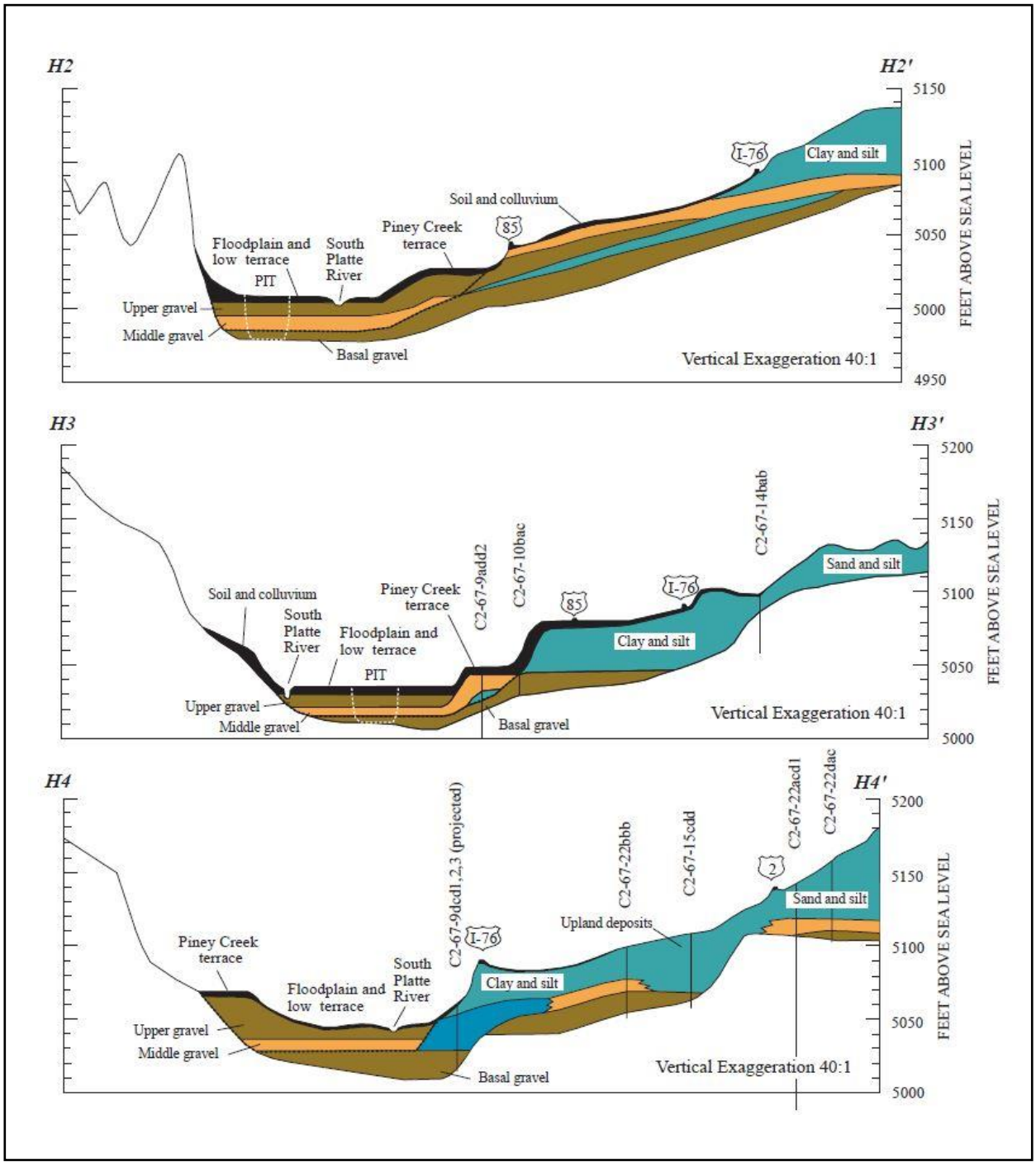

Figure 3: Geologic cross sections showing the alluvial valley of the South Platte River (Lindsey et al, 1998). Cross sections H2, H3, and H4 are located upstream from Brighton, CO at approximate distances of 6, 7.5, and 9 miles respectively.

2.2 Mine Site Area

The chosen study area surrounds an active gravel mining operation located approximately 1.1 km southeast of St. Vrain Creek (Figure 2). The mine site contains an open pit, identified as Pit 116 by the operator, with two active cells. Dewatering to facilitate excavation began approximately in 2012. Parts of the pit are still active in excavation, while other areas have been mined to bedrock. Reclamation has partially begun, and slurry walls have been installed in parts of the pit with little to no gravel extraction. Currently, the pit area is approximately 0.27 km^2 and the mined depth extends below the water table. Monitoring wells clustered near Pit 116, both in the alluvial aquifer and eolian deposits (Figure 2), show a moderate amount of seasonal water table fluctuation (Figure 4). Seasonal fluctuation ranges from 0.4-1.7 m with an average of 0.9 m in all wells installed before pit dewatering.

Borehole and grain size distribution reports from the area adjacent to Pit 116 (on east side, Figure 2 inset map) show gravel deposits thinning to the southeast, towards the edge of the alluvial valley (Terracon, 2008). They also show significant presence of silty and clayey sands above or below gravel deposits in the borehole column. Analysis of the grain size distribution data using the Kozeny-Carman equation yielded hydraulic conductivity estimates ranging from 33.1 – 348.9 m/d with an average of 113.1 m/d (Figure 5). The Kozeny-Carman equation is one of the most commonly used methods to estimate hydraulic conductivity from grain size distribution data in river depositional environments. However, the resulting conductivity values are still characterized by significant uncertainty. Rosas et al. (2014) reported relatively high error margins (approximately -/+ 23 m/d) for this material type due to the varied nature of river alluvial valleys.

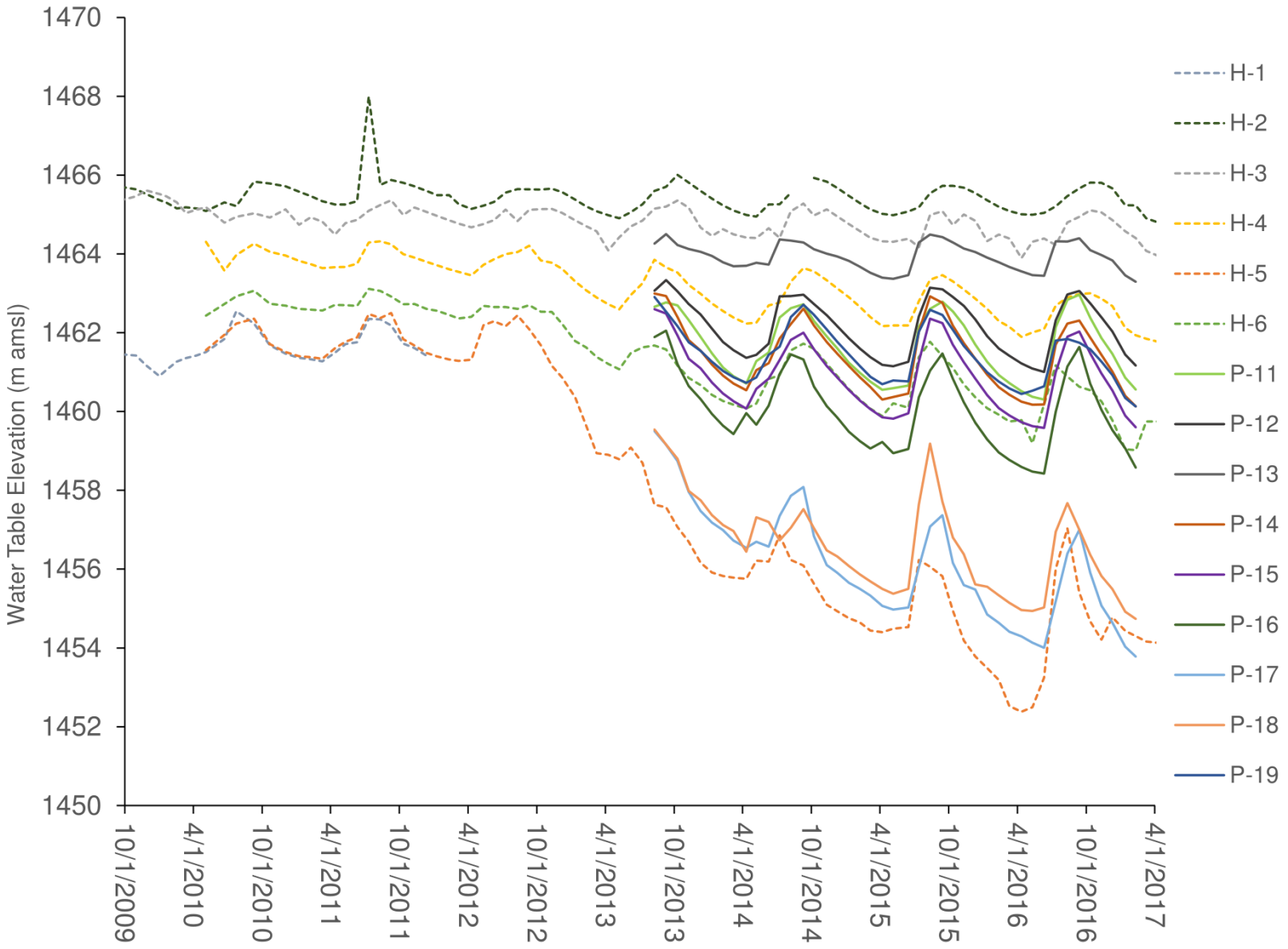

Figure 4: Mine site monitoring well hydrographs from 2009-2017.

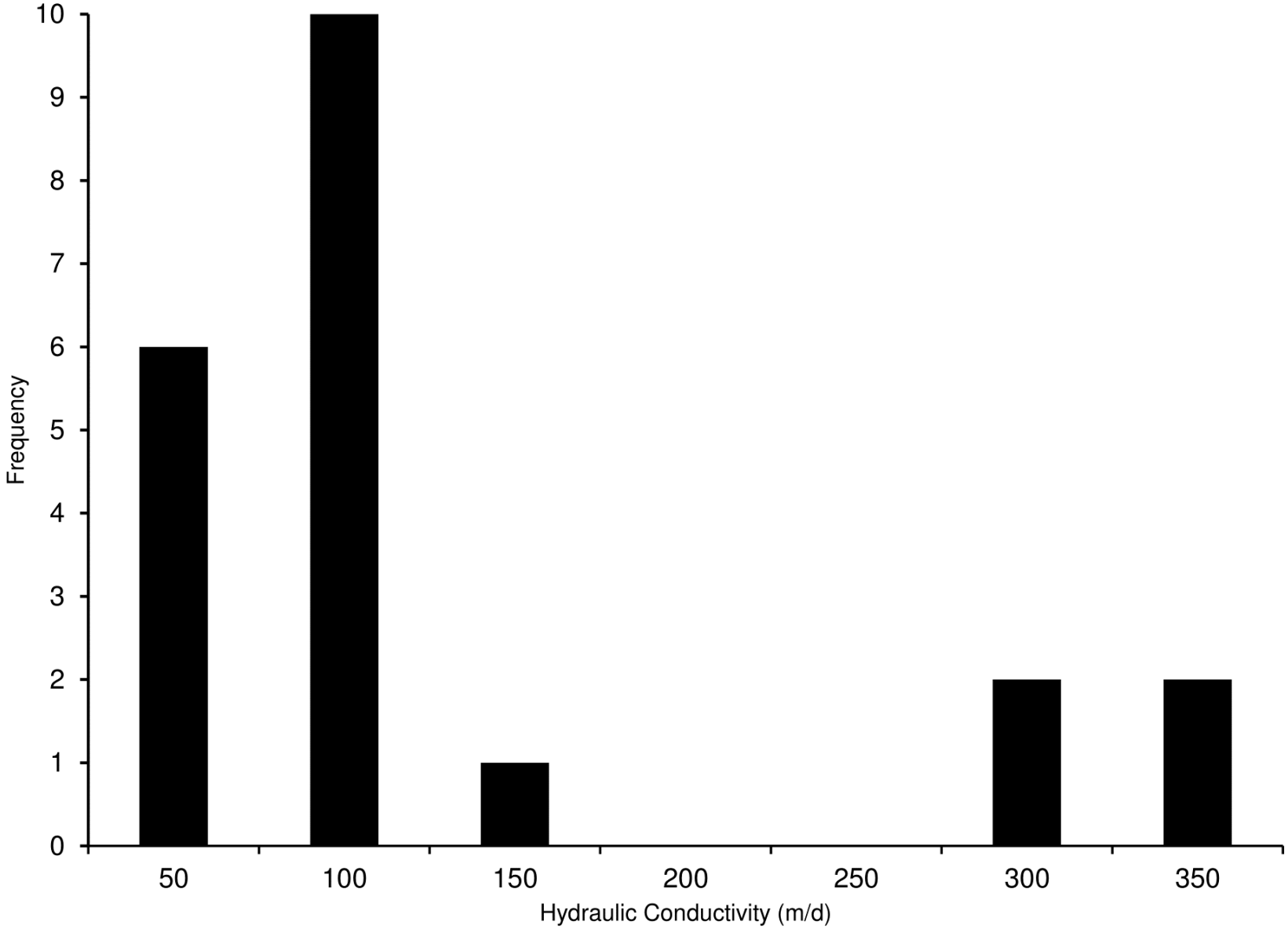

Figure 5: Histogram of estimated hydraulic conductivities based on grain size analyses.

CHAPTER 3: METHODS

This study utilized numerical modeling to analyze the effect of mining on groundwater flow and groundwater-surface water interaction. The numerical model was constructed using MODFLOW-2000 (Harbaugh et al., 2000); Groundwater Vistas version 6 (Rumbaugh and Rumbaugh, 2011) was used as the graphical user interface to facilitate model development.

3.1 Model Design

In order to best represent the conceptual model in numerical space, reasonable boundary conditions and model parameters were assigned to represent the groundwater flow system as described in Chapter 2.

For this study, an initial steady-state model was developed for calibration purposes. Two transient models were also developed, a base case scenario to provide insight into how well the model behaves in comparison with observed data, and a post-mining model scenario to simulate the effects of the lined gravel pit on the water table throughout a representative year. This latter modeling scenario assumes that the liner has been fully installed.

3.1.1 Bedrock Surface

The external boundaries of the alluvial aquifer are formed by the Cretaceous-age bedrock. Accurate representation of the bedrock surface was therefore a key component of the model design. The bedrock surface in this area forms a principal valley carved out of the Pierre Shale and LFH sandstone by Saint Vrain Creek. Smaller bedrock valleys providing underflow to the principal alluvial aquifer can also be found near the Boulder-Saint Vrain confluence (Figure 6).

Previous regional bedrock interpretations conflicted with a relatively new USGS 1-meter digital elevation model (U.S. Geological Survey, 2015). For example, bedrock surface elevations from prior regional interpolation were > 10 m above the land surface in some portions of the study area. Refinement was most needed in the area northwest of Saint Vrain Creek, which was expected considering the abundance of bedrock outcroppings there.

A new bedrock surface was contoured manually and imported into ESRI ArcGIS 10.3 where additional smoothing and editing occurred. The surface was primarily constrained by alluvium thickness measurements (Colton, 1978), and refined using additional data from boreholes in the active mine site area (Terracon, 2008). Bedrock elevation data below the eolian deposits were either very sparse or nonexistent. Previous regional bedrock interpretations were used to better constrain this area (Robson, 1998). In all areas with alluvium at the land surface, bedrock was assumed to be at least 5 meters deep, in order to provide an acceptable match to elevation data within the channel of Saint Vrain Creek. This approach was useful to assure proper simulation of surface water-aquifer exchange in the numerical model. The final interpreted bedrock surface is shown in Figure 6.

3.1.2 Model Domain

Model boundaries are 11.1 km in length by 5.9 km in width, with a total active model area of 45251936 m^2. The grid was rotated clockwise 60 degrees and centered over the principle alluvial aquifer, best accommodating both the northeastern and northwestern principal flow directions. The Saint Vrain Creek flows northeast, entering the model from the southwestern boundary at the approximate location of USGS 06730525 stream gage (Figure 2).

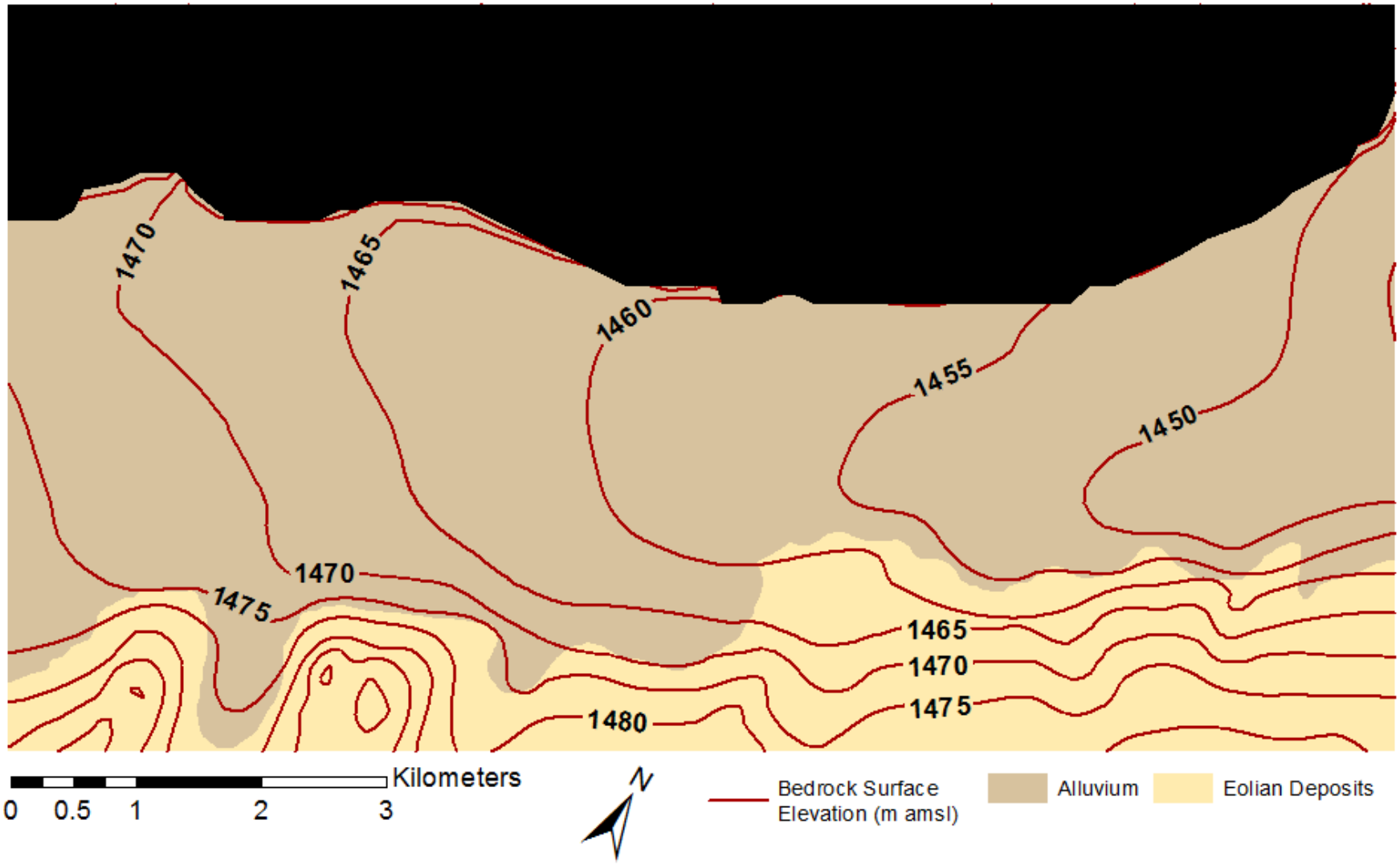

Figure 6: Interpreted bedrock surface within the model area.

The model is 3-dimensional with 2 layers that are identical in size and spatial discretization. Typically, 3D models are used to simulate vertical gradients in hydraulic head (Anderson, Woessner & Hunt, 2015). For this application, inclusion of multiple layers also contributed to model stability by facilitating more successful re-wetting of dry cells. Re-wetting of cells during a simulation can be a source of model instability (Doherty, 2001), particularly for areas of low saturated thickness (e.g., saturated areas outside of the alluvial valley here).

The model grid is irregular with cell sizes ranging from a maximum of 75 by 75 meters to a minimum of 14.81 by 14.81 meters, gradually decreasing in size nearing the gravel pit. A small minimum cell size was chosen to accurately simulate drawdown and mounding around the pit. There is a total of 70784 cells, 59354 of which are active domain.

3.1.3 Model Parameters

Recharge to the water table surface from precipitation was simulated using the recharge (RCH) package (McDonald & Harbaugh, 1988). Assuming ten percent of water travels below the root zone and is not subject to evapotranspiration, a 30-year average precipitation of 35.5 cm/yr[5] was used to calculate a .0001 m/d recharge flux. This equates to 4525 m^3 of recharge to the water table each day over the active model domain. Specific yield was estimated to be approximately 0.25 based on published values for similar sand-gravel material (Johnson, 1963).

This model accommodates three zones of hydraulic conductivity following the conceptual hydrogeologic model (Figure 7): coarse-grained alluvium (gravel and sand), fine-grained alluvium (primarily sand), and eolian deposits. Zone conductivity values were refined during model calibration. The conductivity of the coarse-grained alluvium was constrained by the average of the grain size analyses (113.1 m/d +/- 23 m) and the average of the pumping test

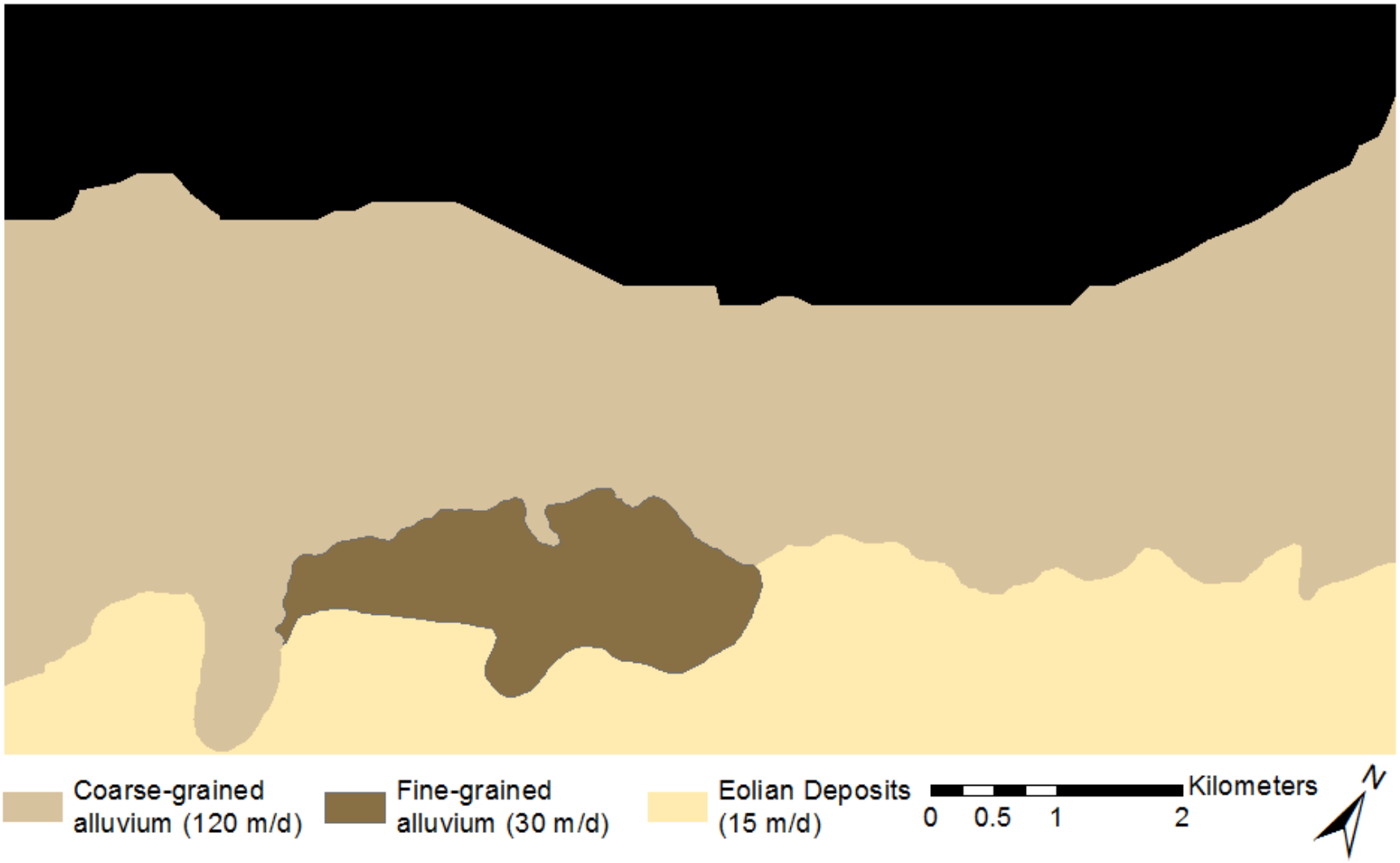

Figure 7: Modeled hydraulic conductivity zonation.

(114.6 m/d) mentioned in chapter 2. Typical gravel conductivity ranges from 86.4 – 864 m/d (Fetter, 2001) revealing this area to have a lower but reasonable range of conductivities.

3.1.4 External Model Boundary Conditions

No-flow boundaries were assigned to cells that coincided with bedrock outcroppings and any eolian deposits cut off from the principal alluvial aquifer. The northeastern edge of the valley is bounded almost entirely by bedrock outcroppings creating a barrier for groundwater flow (Figure 8).

Head-dependent flux boundaries were applied to the model northeast and southwest edges using MODFLOW's General Head Boundary (GHB) package (McDonald & Harbaugh, 1988). GHB cells were used to simulate the inflow and outflow of regional groundwater in the alluvial aquifer and proximal eolian deposits. The GHB package uses a variation of Darcy's Law to calculate flow rates at the boundary based on a specified conductance and external boundary head. For the southwestern inflow boundary, a hydraulic gradient of 0.003 was used to calculate the external boundary heads, whereas a gradient of 0.002 was used for the northeastern outflow boundary heads. These gradients were estimated using wells from the Colorado Division of Water Resources (CDWR) database, which were compiled and contoured to create a water table map.

The well package was used to simulate additional underflow across the southeastern model boundary. Well boundary cells were not placed on bedrock highs (Figure 8) due to the limited saturated thickness and lack of significant groundwater flow in those areas. Individual well recharge rates were targeted to reproduce the estimated 1.5 m in saturated thickness

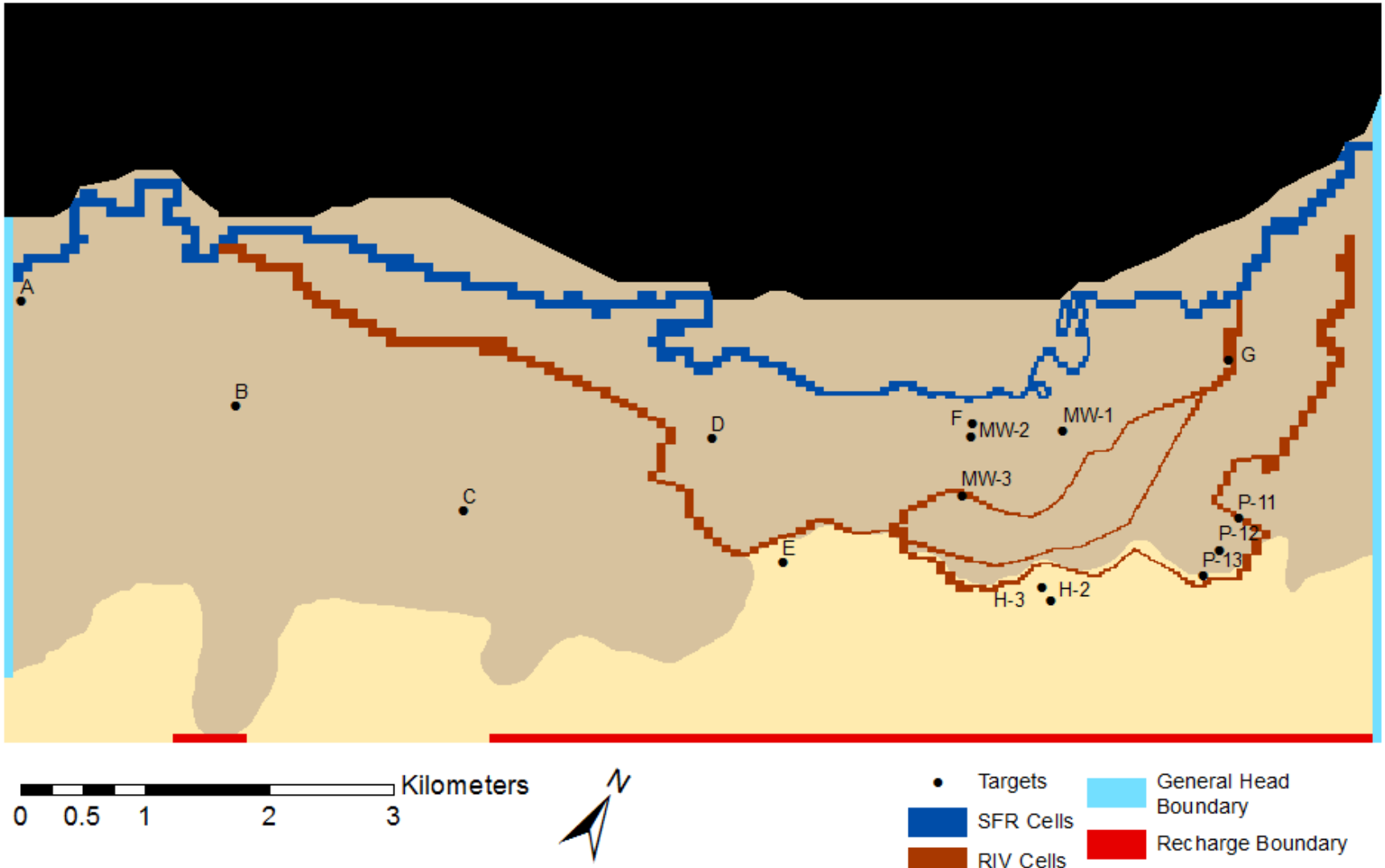

Figure 8: Location of numerical model boundary conditions and calibration targets.

along the boundary. The total modeled volumetric recharge rate across this boundary (8371 m^3/day) was further constrained by the contributing watershed area. Approximately 54.8 km^2 of the Saint Vrain watershed lies behind the southeastern model boundary, yielding an approximate upgradient recharge rate of 0.00015 m/day.

3.1.5 Internal Boundary Conditions

Because of the river-diverting ditch network and the high importance of stream-aquifer interaction in the area, the Streamflow-Routing (SFR1) package (Prudic, Konikow, & Banta, 2004) was used to represent the Saint Vrain Creek. The package computes stream-aquifer interaction using Darcy's Law assuming uniform flow between the stream and aquifer in any given model cell:

$$Q_L = \frac{KwL}{m}(\mathrm{h}_s - \mathrm{h}_a)$$

where Q_L is volumetric flow rate between stream and aquifer (L^3/T), K is the hydraulic conductivity of streambed sediments (L/T), w is width of the stream (L), L is the length of the stream in a given cell (L), m is the thickness of the streambed (L), h_s is the stream stage elevation (L), and h_a is aquifer hydraulic head (simulated water table elevation, L). For all internal model cells with stream-aquifer interaction, h_a, h_s, Q_L, and streamflow are computed internally as part of the model solution. Incoming streamflow is specified for each stress period at the first (upgradient) SFR cell on the western model boundary. These specified streamflow values were based on gaging data from USGS station 06730525.

River gage SVCPLACO near the St. Vrain mouth reports stream depth to width ratios ranging approximately from 1:20 to 1:40 (CDWR, 2017). The range is present because of varying amounts of discharge and stage at different times of measurement. Ratio values

consistently greater than 1 indicate that the St. Vrain Creek is wider than it is deep under both high and low flow conditions. Therefore, stream depth was computed using a version of Manning's equation that assumes a wide rectangular channel, wherein stream depth is assumed much smaller than stream width.

Stream width of 20 m was obtained through measuring the Saint Vrain Creek at multiple points in aerial photography. Streambed thickness is assumed to be a relatively thin 1 m. The conductivity of the streambed material is assumed to be similar to that of the subjacent alluvial aquifer but with higher silt content. Stream width was measured at multiple points along the stream from aerial photography. A value of .06 was used similar to the 'natural flood plain' stream type in Colorado (Jarrett, 1985).

The MODFLOW River (RIV) package was used to model the primary irrigation ditch. RIV cells (Figure 8) are only active during the irrigation season (May to September) in transient scenarios. The ditch was assumed to have 0.15 m of water in it on average, which is within the range indicated by gage data. Additional details on the ditches and Saint Vrain Creek diversions, relevant to transient scenarios performed in this study, are provided in section 3.3 below.

The gravel pit represented in the post-mining transient scenario is assumed to have completed full excavation to bedrock, with a reclamation liner installed around the entire perimeter of the pit. This representation considers the maximum potential effect of the pit liner on the water table by forcing water to flow around the pit, not under it. The pit is modeled as a block of no-flow cells. If installed correctly, pit liners that abide by the state engineer's guidelines for seepage volume into the pit have very low hydraulic conductivity values (SEO, 1999). In a synthetic modeling study, Ronayne and Rach (2018) demonstrated that the pit liner

essentially behaves as a no-flow boundary due to the high contrast in conductivity between the liner and alluvial aquifer.

3.2 Steady-State Scenario

A steady-state model simulates hydrologic parameters, fluxes, and computed heads as constant in time. Head values do not change through time and therefore the aquifer storage properties do not influence the solution (Anderson et al., 2015):

$$S_y \frac{\partial \mathrm{h}}{\partial t} = 0$$

The boundary conditions control the water budget for the solution as there is no water added or released from storage as seen in the equation above. Although groundwater systems are inherently never at steady-state, this can be a reasonable approximation during time periods with relatively constant source/sink fluxes. Steady-state models, in particular, can provide insight into how sensitive the hydrogeologic system is to particular boundary conditions.

It is necessary to pick an appropriate period of time to build the steady-state scenario from, one where boundary conditions change in acceptably small amounts. The general vicinity of the gravel pit displays consistent seasonal head fluctuations (Figure 4) which an extensive local irrigation ditch network contributes greatly to. Boundary conditions for the steady-state scenario (Figure 8) were built around data from the February to April months, minimizing the impact of the seasonal irrigation network and spring snow melt affecting the Saint Vrain Creek's discharge.

3.3 Transient Scenarios

Transient models simulate stresses changing at varying points in time (e.g. pumping rates or streamflow variability) through use of stress periods. The beginning of a new stress period generally denotes a change in one or more stresses to the model. Head values in a 3-dimensional model change through time as described mathematically in the standard groundwater flow equation (Anderson et al, 2015):

$$\frac{\partial}{\partial x}\left(K_x \frac{\partial h}{\partial x}\right) + \frac{\partial}{\partial y}\left(K_y \frac{\partial h}{\partial y}\right) + \frac{\partial}{\partial z}\left(K_z \frac{\partial h}{\partial z}\right) = S_s \frac{\partial h}{\partial t} - W^*$$

where K is hydraulic conductivity (L/T) (subscripts *x, y, & z* denote anisotropy), S_s is specific storage (1/L), and W^* is a source/sink term that represents internal recharge or discharge to/from the aquifer (1/T).

Steady-state model hydraulic heads were used as the initial condition for the transient scenario. Twelve stress periods, representing each calendar month of the year, were established to discretize two time-varying stresses to the system: discharge in Saint Vrain Creek and irrigation ditch status (active or inactive). Because of the seasonality in this area and the large differences seen in stream discharge data during the summer months (Figure 9), representative monthly mean values were calculated for Saint Vrain Creek discharge and diversions. For example, discharge values in February from each year were all included in the mean (2014, 2015, 2016, etc.) in order to provide a representative year for stress period inputs. All respective monthly mean data excludes observations from the 2013 Oct-Dec months due to the extreme flooding in the Saint Vrain Watershed that September (Gochis et al., 2015; Rathburn et al., 2017). In addition to the irrigation ditches, diversions from the Saint Vrain Creek are also active from May to September and follow the respective monthly mean method described above. Diversion data were obtained from the head gate of the primary irrigation ditch (CDWR, 2017).

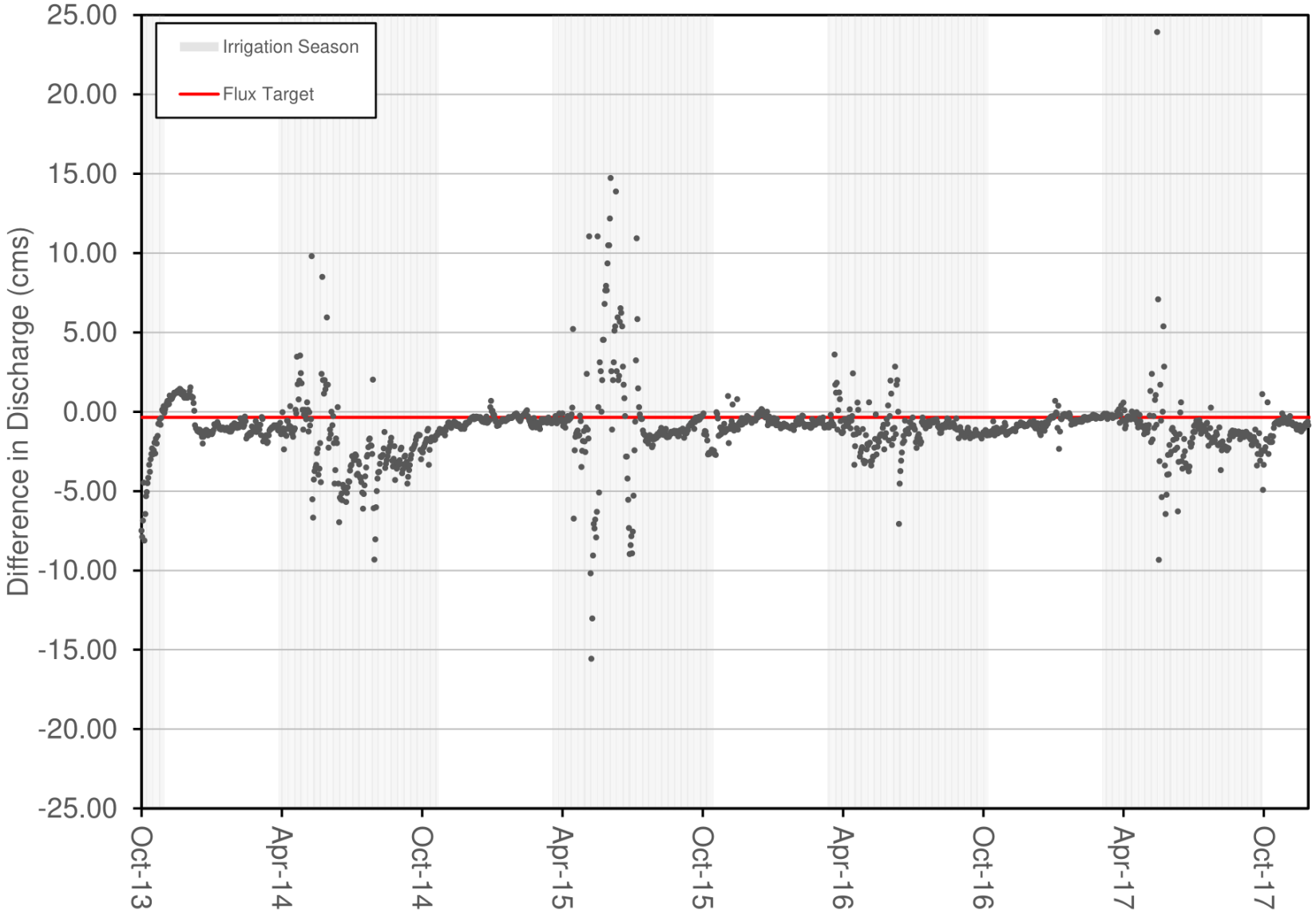

Figure 9: Difference in mean daily streamflow between gages on the Saint Vrain Creek. Values are obtained by subtracting CDWR SVCPLACO gage (downgradient) discharge values from USGS station 06730525 discharge values (upgradient).

3.4 Performance & Calibration

Evaluation of the steady-state model was done using measured hydraulic heads (head calibration targets) from three sources and a flux target for the Saint Vrain Creek. For this study, the parameters focused on for adjustment during calibration included the aquifer hydraulic conductivity and GHB conductance. These two parameters had the highest amount of influence on simulated heads and baseflow in the Saint Vrain Creek.

Residual statistics from head calibration targets are useful tools to assess model performance. Residuals are found from observed head minus simulated head. A mean error (ME) of residuals close to zero is an indicator of little bias. Mean absolute error (MAE) takes the mean of the residual absolute values, measuring the magnitude of errors without considering their direction (positive or negative). Compared to ME, it is usually higher and is a better indicator of goodness-of-fit. The residual Root Mean Squared Error (RMSE) is more susceptible to outlier residuals than MAE, and as a consequence, is usually higher than MAE. There is no set acceptable standard for these values, except they should be minimized (Anderson et al., 2015). Acceptable values for residual statistics largely depend on modeling objectives. Modeling objectives for this study include recreating the general pattern of groundwater flow, as well as producing a calibrated model that can be used for forecasting.

In addition to head calibration targets, baseflow in the Saint Vrain Creek was used to establish a flux target of 0.34 m^3/s (net groundwater discharge to the river, or amount of gain in streamflow, over the model area) for the non-irrigation season. To obtain this flux target, the mean discharge of all the non-irrigation months was taken at both stream gages and differenced. October and November were excluded from this calculation because the hydraulic heads and streamflow are still recovering from the irrigation season during those two months. Between the

two stream gages, only 68% of the Saint Vrain Creek is in the model area; this factor was applied to obtain the final flux target (0.34 m^3/s).

Both the base case and post-mining transient scenarios were run through multiple years in order to distance solution values from the initial condition. The model was considered stabilized (i.e., converged on a steady-periodic solution) when the difference in head from a specified date was less than 0.1 m between successive simulated years. (e.g. Oct 1st head value subtracted from Oct 1st head value of the following simulation year).

Although a separate transient calibration was not performed, the base case was compared against the flux target and select monitoring wells near the pit to assess performance. Wells H-2, H-3, P-11, P-12, and P-13 (Figure 2) were selected to compare simulated heads with observed heads for a representative year. Head observations were averaged following the respective monthly mean method mentioned above.

In order to better evaluate drawdown and mounding associated with the pit liner, six observation points were placed around the pit in transient scenarios (Figure 10). Two of these (N1 and N2) are downgradient of the pit in the principal direction of groundwater flow, placed to best assess shadow drawdown. Two are placed upgradient from the pit (U1 and U2) to assess mounding in the coarse-grained alluvial zone, and another two (S1 and S2) are placed to assess mounding near the edge of eolian deposits. Observation points with '1' are located 100 m from the pit, and points with '2' are 400 m away from the pit. These observation points compared simulated heads from both the base case and post-mining transient scenarios to assess the difference (i.e., to determine the influence of lined pit) throughout the representative year.

Head values from the post-mining scenario were subtracted from head values in the base case scenario during their respective times (e.g. December heads were subtracted from December

heads). This gives water table elevation change produced solely from the pit liner and how it varies through the year.

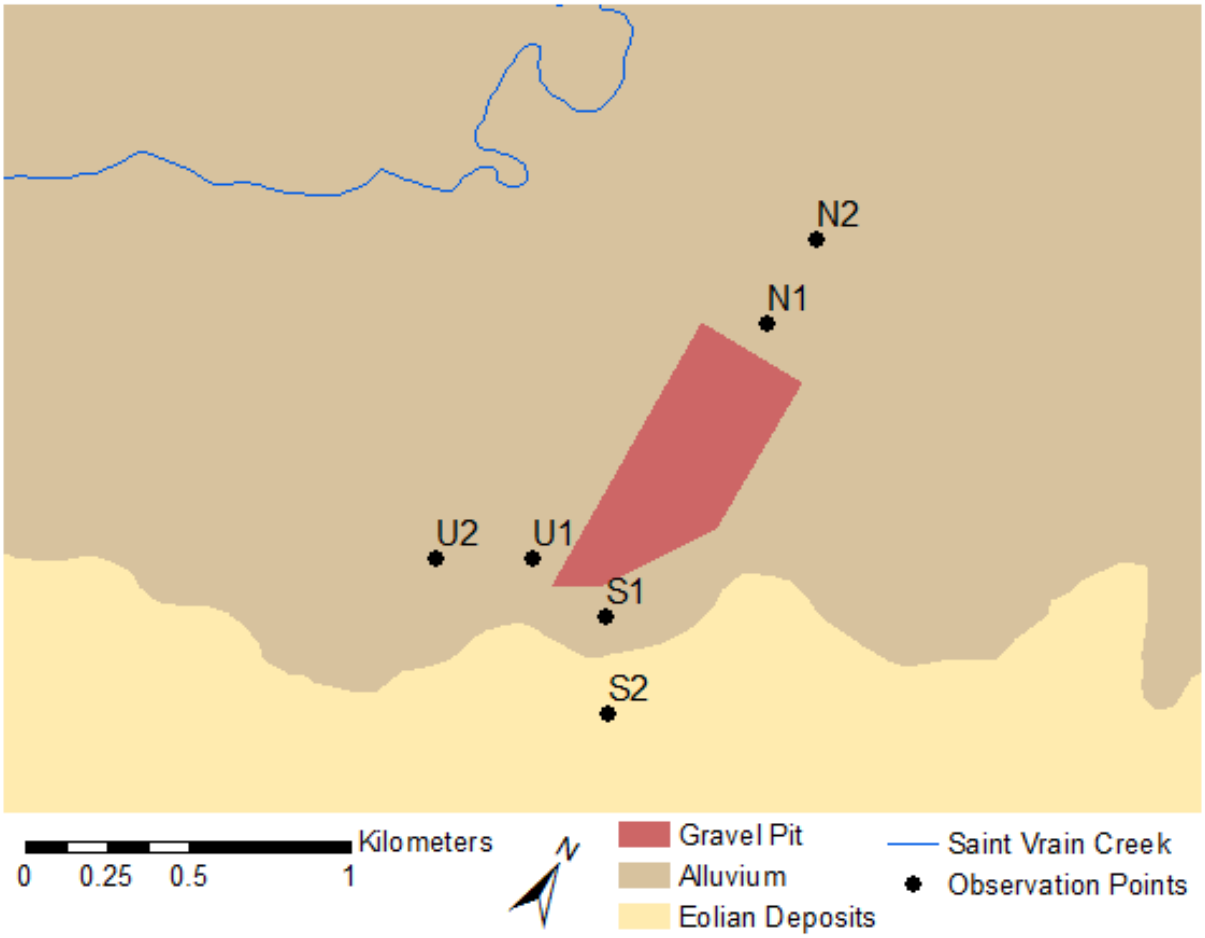

Figure 10: Locations of selected observation points used to compare transient scenarios.

CHAPTER 4: RESULTS

4.1 Steady State Scenario

The major objective for the steady-state model was to reasonably predict aquifer hydraulic heads and Saint Vrain Creek baseflow, and also provide a basis for transient modeling through calibrated aquifer properties and boundary conditions. Steady-state head contours mimic the pattern of groundwater flow from other hydrogeologic studies of this area (Figure 11). Average hydraulic gradients are 0.0026 to the northeast and 0.015 northwest in the alluvial aquifer and eolian deposits respectively. These values are comparable to the interpreted hydraulic gradients from the most recent regional study, 0.0024 NE and 0.014 NW (Robson et al., 2000).

The steady-state model produced an ME of -0.024 m indicating the simulated values are generally not biased high or low. MAE and RMSE are 0.77 m and 0.97 m respectively. When taking into account head solutions across the entire model, MAE divided by the range of observed heads produces a model error of 3.69% (Table 1). These residual statistics indicate that the model is reasonably well calibrated, and groundwater flow conditions within the study area are reasonably reproduced.

A scatterplot of simulated versus observed hydraulic heads is shown in Figure 12. Bias of the model is considered low when points are equally scattered along the 1:1 line. Scatterplots can also reveal bias at certain head elevations in the model. For example, above an elevation of 1470 m, simulated heads tend to be lower than the observed hydraulic heads. Overall, the calibration targets are well distributed along the 1:1 line.

The simulated groundwater discharge into Saint Vrain Creek is 0.25 m^3/s in the steady-state model, approximately 25% lower than the target discharge. The model has a slight bias towards under predicting the hydraulic heads (Table 1, ME, and Figure 12), which contributes to lower simulated groundwater discharge into the Saint Vrain Creek. This may be attributable to lingering effects from the irrigation season (i.e., the non-irrigation season may not be long enough to achieve steady-state conditions).

Table 1: Calibration statistics and list of calibration targets for steady-state model.

Calibration Targets		
	Date Measured	**Residual**
USGS Historical GW Levels		
A	5/4/1977	-0.97
B	5/4/1977	1.08
C	4/29/1977	1.67
D	4/29/1977	-0.11
E	4/28/1977	0.35
F	5/11/1977	0.09
G	5/11/1977	-1.30
Owens Bros. Site		
MW-1	4/5/2002	-1.55
MW-2	4/5/2002	-1.52
MW-3	4/5/2002	-0.07
Pit 116 Area		
P-11	2/10/2014	0.19
P-12	2/10/2014	0.52
P-13	2/10/2014	1.51
H-2	2/7/2014	-0.44
H-3	2/7/2014	0.19

# of Wells	Mean Error (m)	Mean Absolute Error (m)	Root Mean Squared Error (m)	Minimum Residual (m)	Maximum Residual (m)	Observed Head Range (m)	Mean Absolute Error / Range (%)
15	-0.024	0.77	0.97	-1.55	1.67	20.86	3.69

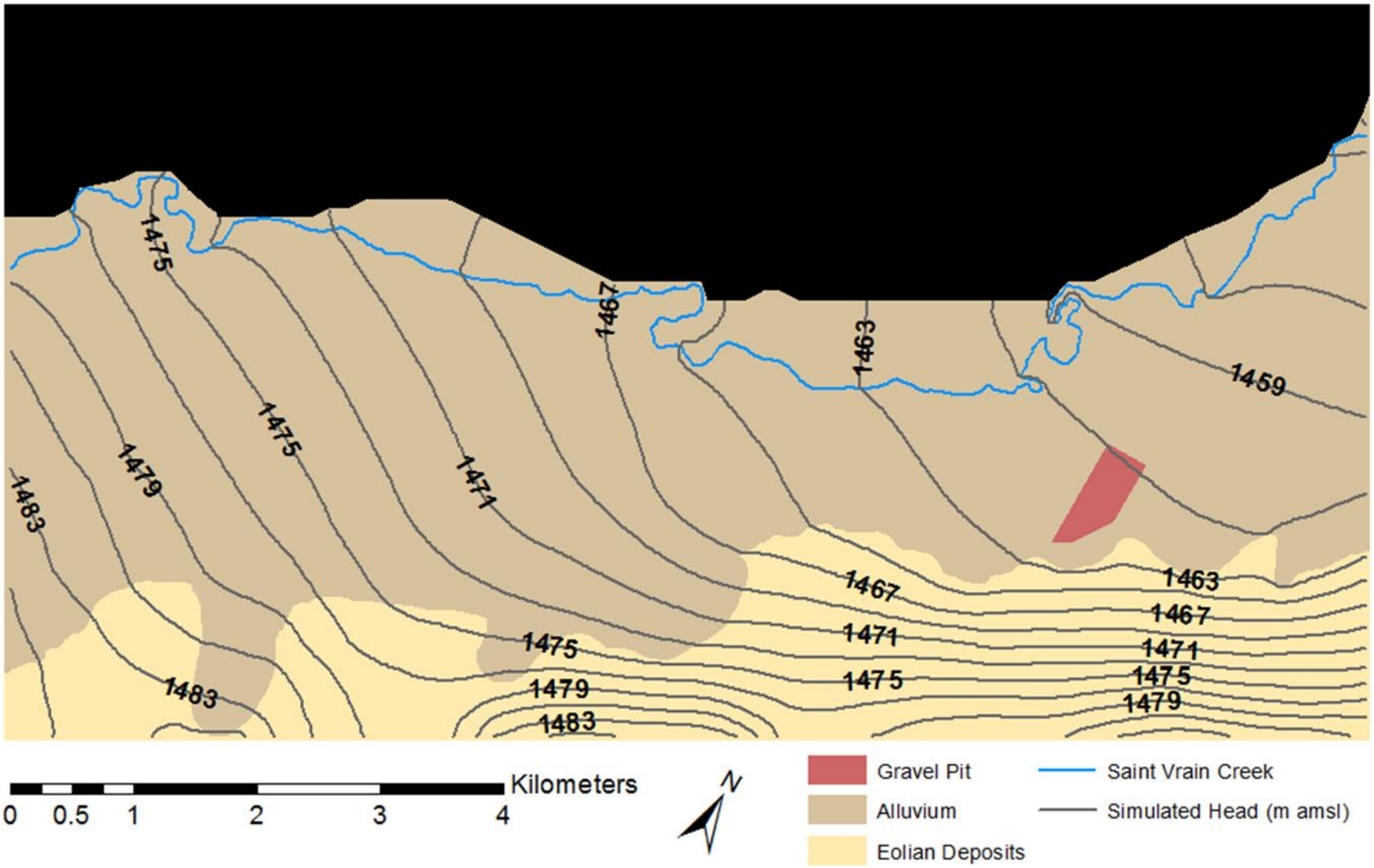

Figure 11: Simulated, pre-mine water table elevation for calibrated steady-state model. Contour interval is 2 meters.

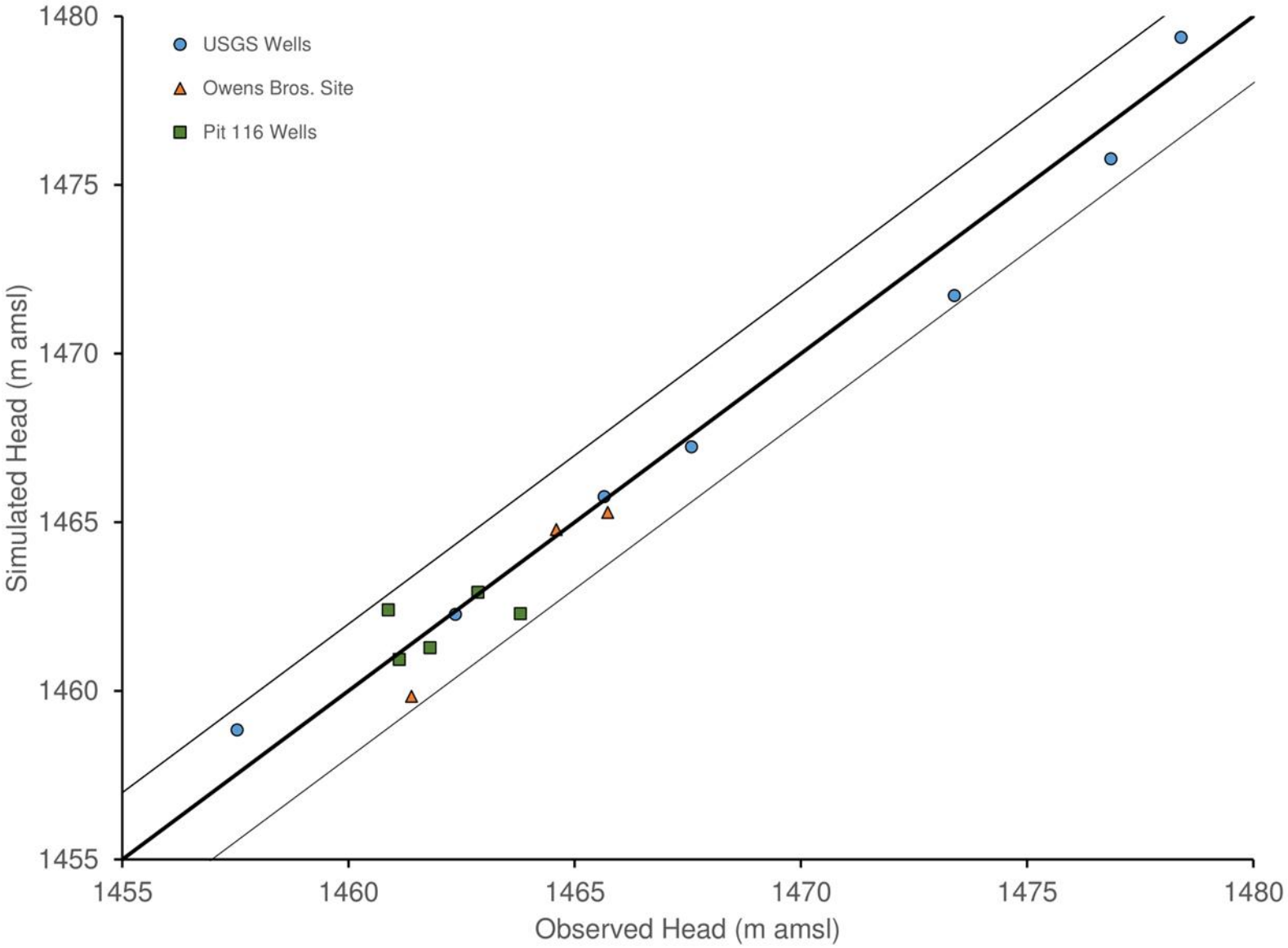

Figure 12: Simulated versus observed hydraulic heads for steady-state model. Solid black line is the 45-degree line. Gray lines provide 95% confidence intervals for the hydraulic head targets.

4.2 Base Case Transient Scenario

Boundary conditions from the steady-state model were modified to introduce seasonal stresses in the form of varying streamflow and irrigation. Simulated heads around the gravel pit follow a predictable seasonal pattern similar to those seen in observed heads (Figure 13). Predictably, simulated heads hit a yearly low at the end of April before irrigation is activated in May and hit a yearly high at the end of irrigation season in September. A distribution of monthly residuals at each of the five monitoring wells shows the model is more often overpredicting heads near the pit than underpredicting (Figure 14). However, a significant portion of the residuals center around zero show the model is not strongly biased in this area.

At wells H2 and H3, the simulated intra-annual range in heads closely matches the observed head range before nearby mine dewatering starts in 2012 (Table 2). For wells P-11 and P-12, simulated head ranges are nearly half of observed head ranges in water years 2014 & 2015. However, these data were affected by the nearby pumping and observed head ranges are expected to be larger than normal. Baseflow to the Saint Vrain Creek during the non-irrigation

Table 2: Range of hydraulic head observed in five monitoring wells from water years 2010 to 2015 (average values calculated from water years before nearby mine dewatering began). Simulated range in head at each location is included for comparison.

	(m)	H2	H3	P-11	P-12	P-13
Pre-mine dewatering	WY 2010	0.7	0.8	-	-	-
	WY 2011	0.6	0.9	-	-	-
	WY 2012	0.7	0.5	-	-	-
Active mine dewatering	WY 2013	0.8	1.1	-	-	-
	WY 2014	1.1	0.9	2	1.7	0.7
	WY 2015	0.9	1	2.2	2	1.1
	Simulated	0.6	0.7	1.1	1.2	1.4
Average Observed Head Range						0.7

season was much closer to the flux target of 0.34 m^3/s. Transient baseflow ranged from 0.33 m^3/s in December and January decreasing to 0.27 m^3/s in April for an average of 0.31 m^3/s. Both of these factors show the transient model is simulating a representative seasonal water table fluctuation near the gravel pit and a representative average baseflow to the Saint Vrain Creek.

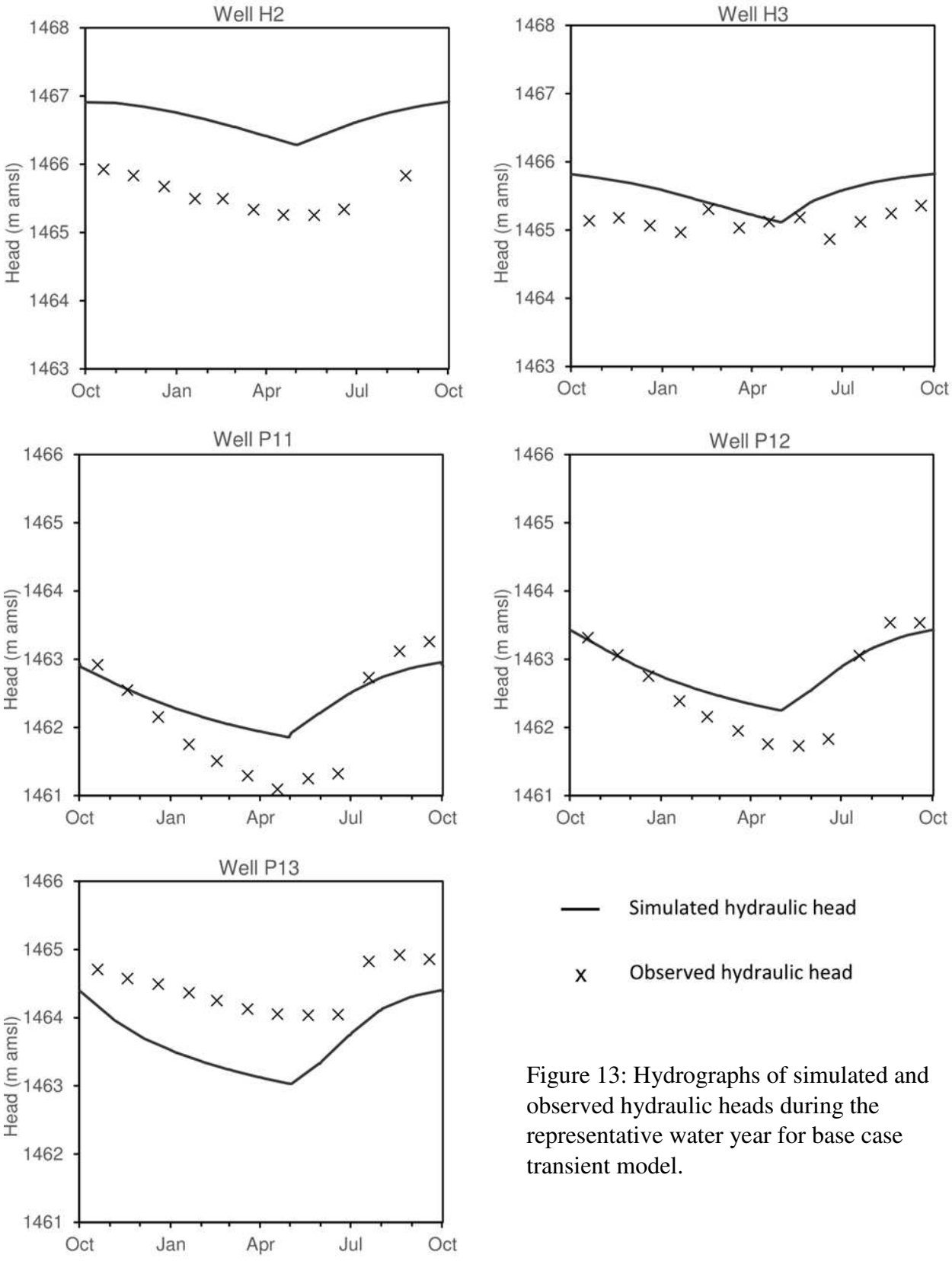

Figure 13: Hydrographs of simulated and observed hydraulic heads during the representative water year for base case transient model.

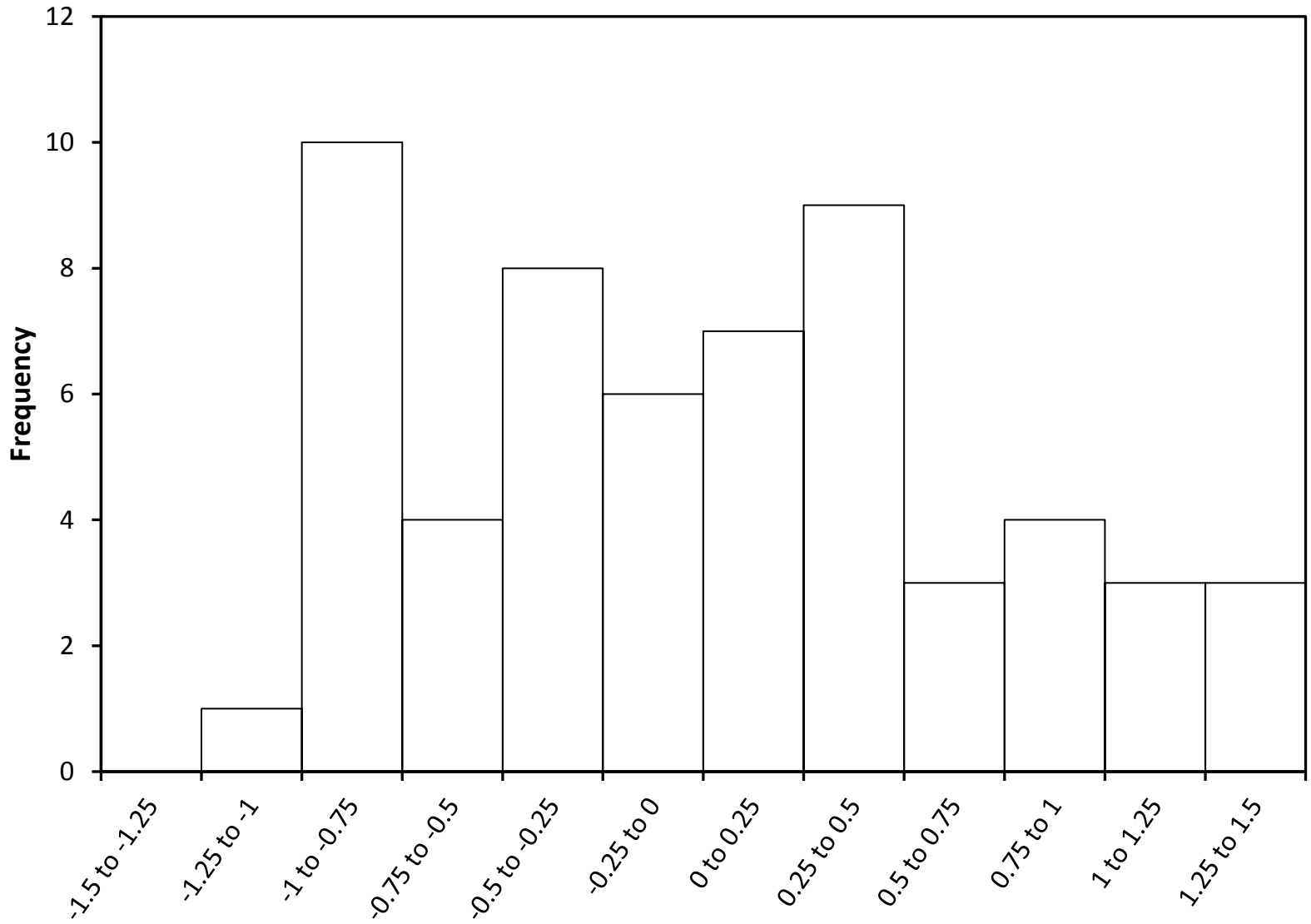

Figure 14: Histogram of residuals in the base case transient run. Residuals were calculated at each of the five monitoring wells (H2, H3, P11, P12, P13), once a month for the representative year.

4.3 Post-Mining Transient *Scenario*

By including no-flow cells within the open pit, this scenario was designed to consider the effects of a low-permeability liner. Changes, or hydraulic head differences, associated with the pit liner were calculated by subtracting the simulated heads in this scenario from the corresponding simulated heads (at same time) in the base case scenario. The difference in simulated hydraulic heads around the gravel pit varies throughout the year (Figure 15 and 16).

Water table elevation change is seen on all sides of the pit. Mounding is observed west and south of the pit while shadow drawdown is observed north of the pit. The extent of mounding and shadow drawdown follows a cyclic pattern with yearly lows at the end of irrigation season and yearly highs just before irrigation begins suggesting. At the observation points (Figure 15), the highest water table mounding occurs in S1 southeast of the pit; the magnitude of mounding at this location reaches 0.5 m and then sharply drops to less than 0.1 m. An equal distance away west of the pit is point U1, which sees a range of approximately 0.1 m-0.25 m. Water table drawdown, while still cyclic in nature, experiences less drastic fluctuations throughout the year. Point N1 experiences maximum drawdown values of 0.3 m during the non-irrigation season and values as low as 0.2 m during irrigation.

Mounding and drawdown also vary spatially throughout the year (Figure 16). In March, simulated mounding of 0.2 m is observed nearly 175 m away from the pit to the west in the alluvial aquifer and 750 m to the southeast in the eolian deposits. Drawdown of 0.2 m occurs 250 m north of the pit in the alluvial aquifer. When irrigation ends in September, water table elevation change or ΔWTE (i.e., the simulated difference between scenarios) has shrunk significantly. At distances greater than 25 m away from the pit, mounding is less than 0.1 m in both the western and southeastern directions, resulting in an almost complete disappearance of

mounding. The drawdown 0.2 m line is now 150 m away from the pit, and the size of the drawdown influence 0.1 m and above shrunk to 47% of its size in March.

4.4 Stream-Aquifer Interaction

Simulated water exchange between Saint Vrain Creek and the alluvial aquifer was compared for the transient scenarios because water table disturbance contours (Figure 16) show possible effects on the river. The river is approximately 750 m west of the pit. Differences in stream-aquifer interaction between the two scenarios occurred in stretches of the river near or downstream from the pit, leading to a net increase in groundwater discharge to the river for the post-mining (lined pit) scenario. However, these differences were negligible, amounting to only 0.11% of the total streamflow in December and 0.06% of the total streamflow in March. Stream-aquifer interaction was only compared for December and March given that the differences between scenarios (i.e., the effects of pit liner) are greatest during the non-irrigation season.

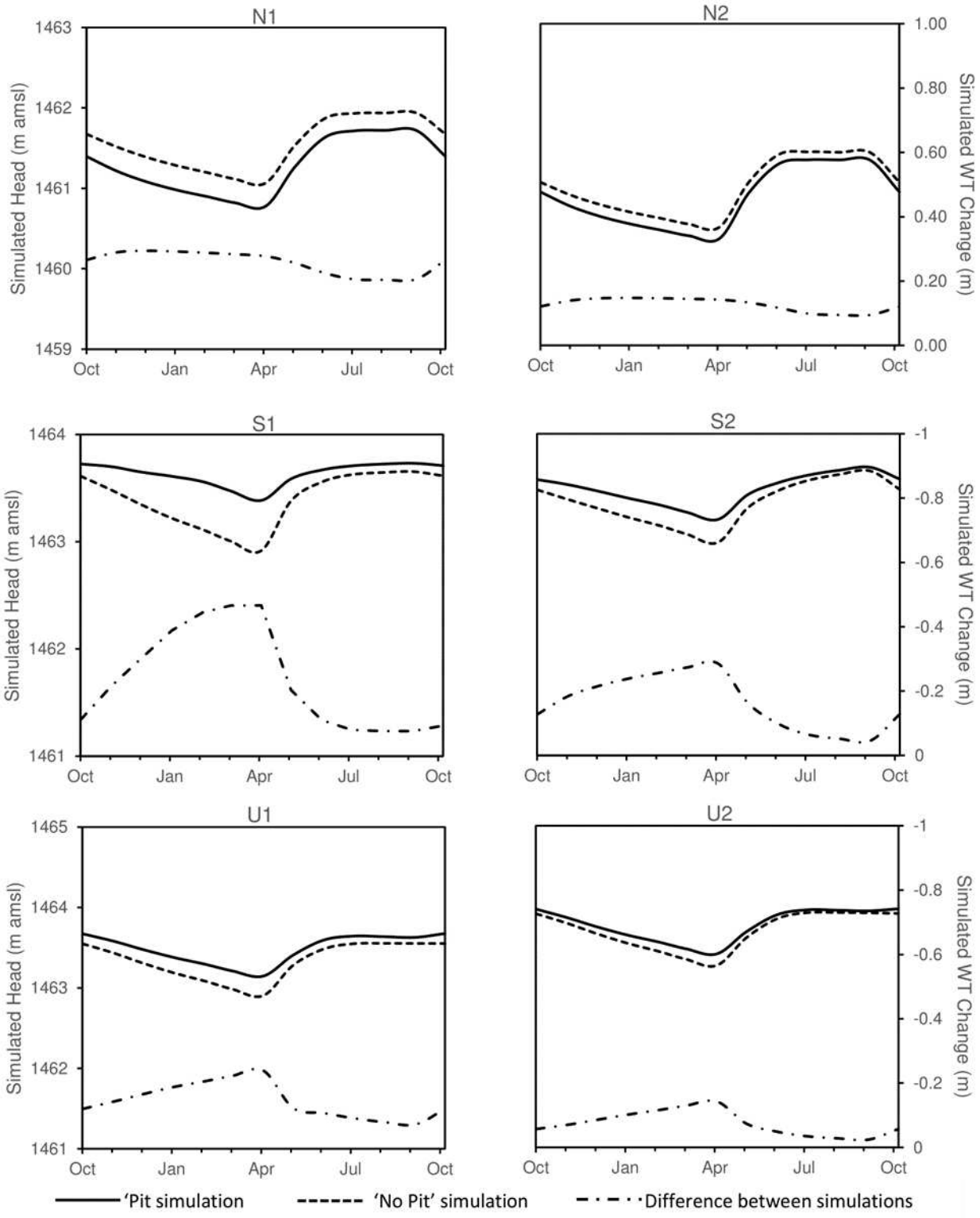

Figure 15: Simulated hydraulic heads and head difference (amount of water table change for post-mine scenario with liner installation) at selected observation points shown in Figure 10. Negative values indicate mounding while positive values indicate drawdown.

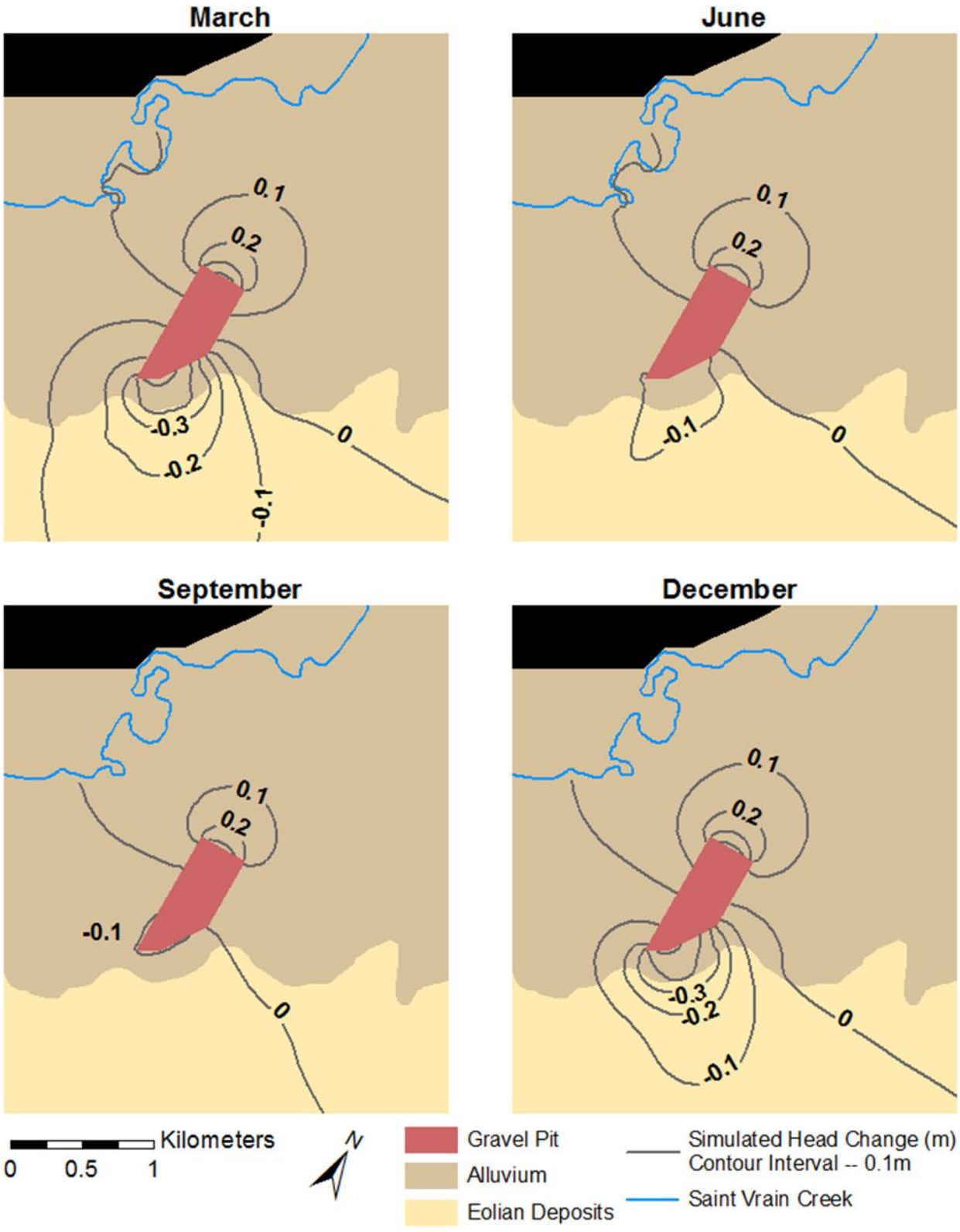

Figure 16: Simulated water table change at the end of four months of the year. Negative values indicate a predicted water table increase (mounding), whereas positive values indicate a decrease in the water table elevation (drawdown).

CHAPTER 5: DISCUSSION

Sand and gravel deposits within the Saint Vrain alluvial valley are an important source of aggregate, and the underlying alluvial aquifer is an important water resource, particularly for irrigated agriculture in this area. Through the development of a refined conceptual hydrogeologic model and a numerical model, this study evaluated the potential impacts of lined aggregate pits relative to other seasonal factors that influence groundwater flow patterns. The study area displays a consistent intra-annual head fluctuation around the gravel pit before nearby pumping in 2012 (Figure 4) and is never truly in steady-state. For initial steady-state model development, care was taken to select the February through early April period deemed most representative of steady conditions.

All head calibration targets were assumed to follow this consistent pattern, with relatively stable heads during February-April, but this may not be the case everywhere in this aquifer. Four of five observation wells used to evaluate the base case transient scenario confirmed the model's ability to reproduce seasonal fluctuations in hydraulic head for a representative year (Figure 13). Simulated head for well H-2 followed the rise and fall of observed head closely, predicting 2010-2012 ranges of heads with 0.1 m of error (Table 2). Observed head data from well H-3 does not show a seasonal pattern similar to the other wells. Larger observed head ranges from 2013 and forward can be attributed to nearby mine dewatering affecting local gradients.

Wells P-11, P-12, P-13 all showed larger simulated fluctuations in seasonal head than the H wells (Table 2). Larger head fluctuations can also be seen in observed head data at these wells which is consistent with the idea the high conductivity alluvial zone will see larger ranges in head. However, observed head ranges at these wells are 50-81% larger than their simulated

equivalents with 0.9 m as the highest error. Unfortunately, data collection for P-series wells started in late 2013 after nearby mine dewatering started and likely affected these wells. Starting in 2013, observed head ranges also increased at the H-series wells, so it is reasonable to assume ranges increased for P-series wells as well. If there were observed head data prior to 2013 at P-series wells, the margin of error would likely be smaller.

Observed data for P-series wells also show aquifer response to irrigation is approximately 2 months later than the model is predicting (Figure 13). This behavior is not seen in either of the H-series wells. In all three P-series wells, there is a significant jump in observed head between the June and July readings. Simulated head values quickly begin rising in May when irrigation becomes active in the model. This could be the result of a number of factors, including heterogeneity in aquifer properties and/or variation in irrigation water application.

The spatial extent and magnitude of groundwater disturbance around the gravel pit is influenced by the extensive ditch irrigation network, evidenced by the timing of the high and low of ΔWTE. Maximum disturbance occurs just before irrigation begins and minimum disturbance occurs when irrigation is ending, suggesting irrigation contributes more to groundwater rise and fall than does the pit liner.

From the results of the transient scenarios clearly indicate that the liner affects water table elevations in the immediate vicinity (less than 50 meters away) of the pit. However, the magnitude of disturbance is less than pre-mining seasonal head fluctuations associated with natural and irrigation-related factors. During the period of time with maximum pit-liner influence, the highest values of mounding and drawdown values reach just over 0.5 m and 0.4 m, respectively, and these changes are observed over relatively small areas. During the irrigation season, when the differences between scenarios is minimal, mounding and drawdown reach just

over 0.1 m and 0.2 m respectively. When comparing these results to the average observed head range of 0.7 m before mine dewatering (Table 2), groundwater disturbance associated with the pit liner ranges from 14-71% of seasonal head fluctuation at its respective maximum and minimum.

Simulated changes in water-table elevation caused by the liner quickly dissipate with distance from Pit 116 (Table 3). Eolian deposits on south side of the pit experience maximum mounding that corresponds to 55.7% of the seasonal head range at 100 m which drops off to 34.3% at 400 m. On the other hand, the alluvial aquifer west of the pit experiences maximum mounding that is 22.9% of the seasonal range at 100 m and 17.1% at 400 m. During the irrigation season, the water contribution from ditches almost entirely overshadows any effect the pit liner has on the upgradient side in both principal groundwater flow directions.

The spatial extent and magnitude of groundwater disturbance is controlled by factors other than the irrigation present in the area. Mounding on the south side of the pit is more spatially extensive than mounding on the western side at certain times during the year (Figure 16). The south side is directly upgradient relative to the principal direction of groundwater flow

Table 3: Maximum and minimum water-table elevation change (ΔWTE) observed at six observation points around the gravel pit. Negative values indicate mounding whereas positive values indicate drawdown. Percentages are calculated from an average observed head range of 0.7 m.

(m)	N1	N2	S1	S2	U1	U2
Maximum ΔWTE	0.31	0.15	-0.47	-0.29	-0.24	-0.14
Minimum ΔWTE	0.22	0.09	-0.08	-0.05	-0.08	-0.02
Range	0.09	0.06	0.39	0.24	0.16	0.12
Distance from pit	100	400	100	400	100	400
Max Disturbance % of Avg. Seasonal GW Range	12.9%	8.6%	55.7%	34.3%	22.9%	17.1%

from eolian deposits into the alluvial valley, with a simulated hydraulic gradient of 0.014. On the other hand, the western side of the pit is in the upgradient direction relative to the northeasterly flow direction through the alluvial aquifer, which is characterized by a simulated hydraulic gradient of 0.0022. However, the alluvial hydraulic gradient shifts slightly during irrigation season.

The southern side of Pit 116 is also near (~ 250 m) a hydraulic conductivity zone border. Conductivity changes from 120 m/d around the pit to 15 m/d in the eolian deposits. ΔWTE contours of 0.1 m are similar distances away both on the western and northern sides of the pit but are much further away on the south side. This suggests that a lower hydraulic conductivity contributes to higher magnitude and more spatially extensive mounding, and that conductivity is a major control on how disturbance is propagated.

Drawdown on the north side of Pit 116 is much more consistent in both magnitude and spatial extent than mounding. Similar to the south side of the pit, this area is in close proximity to two branches of the primary irrigation ditch. However, large seasonal differences in groundwater disturbance are not witnessed. Irrigation has a smaller effect on the magnitude of drawdown, perhaps due to differing flow paths from irrigation ditches in this downgradient area. In the case of mounding on the south side of Pit 116, the irrigation ditches are directly within the affected area.

While the pit liner had a clear impact on the simulated water table elevation (locally near the pit), the impact on stream-aquifer exchange was negligible. The simulated impact on the Saint Vrain Creek (i.e., change in baseflow associated with liner installation) never exceeded 0.11 % of the total streamflow. The water-table increase in the immediate vicinity of the creek was less than 0.1 m, and was closer to zero in some areas (Figure 16). If the gravel pit were

closer to the Saint Vrain Creek, it is reasonable to assume the pit would have a greater impact on stream-aquifer interaction.

CHAPTER 6: CONCLUSIONS AND RECOMMENDATIONS

6.1 Conclusions

Gravel pits with liners act as a boundary to groundwater flow creating relative mounding on the upgradient side and drawdown on the downgradient side. These effects were evaluated for a study area along Saint Vrain Creek in Colorado, in an area where open-pit gravel mining has intersected the alluvial aquifer. Transient numerical groundwater modeling was performed to quantify the potential influence of a liner surrounding an active pit. Results for a post-mining, lined-pit scenario were compared to a base case (pre-mining) scenario. They revealed ΔWTE around the pit was variable throughout the year, highly dependent on a local irrigation ditch. Maximum effects are seen in April just before irrigation and minimum ΔWTE at the end of irrigation in September, creating a seasonal pattern produced by the lined pit.

Hydraulic conductivity was a key factor in controlling the magnitude and especially the spatial extent of groundwater disturbance. Lower conductivities associated with eolian deposits led to more spatially extensive groundwater mounding on the south side of the pit.

The installation of a lined pit, while it altered local heads, had little effect on the nearby river. Simulated stream-aquifer interaction changed by a maximum of 0.11% of the river's total streamflow value during the non-irrigation months.

6.2 Recommendations for Future Work

This study helped answer questions about the effects a particular gravel pit on the local water table and also reinforced the fact that hydraulic conductivity is a major driver in controlling the extent of those effects. Recommendations for further research deal with two main

questions. Groundwater disturbance has been shown to be spatially extensive for a single, lined pit, but alluvial valleys often have more than one excavation site. Future research should explore the cumulative effects of multiple lined gravel pits on an alluvial aquifer. Another major question is the potential impact of these pits on groundwater-surface water interaction. Alluvial valleys are sources of high quality aggregate making them prime targets for gravel pit development. Pits closer to the river may produce a greater effect on stream-aquifer interaction, though it remains an open question if this effect would be significant relative to total streamflow. Both of these topics are a logical next step for studying the effects of lined gravel pits on the local water table and may provide important additional insights.

WORKS CITED

Anderson, M. P., Woessner, W. W., & Hunt, R. J. (2015). *Applied groundwater modeling: Simulation of flow and advective transport*. London: Academic Press. pp. 381.

Arnold, L. R., Langer, W. H., & Paschke, S. S. (2003). *Analytical and numerical simulation of the steady-state hydrologic effects of mining aggregate in hypothetical sand-and-gravel and fractured crystalline-rock aquifers* (No. 2002-4267).

AWES (American Water Engineering Services, LLC). (2015). *Dewatering Evaluation Report* (Tech.). Unpublished.

CDM Smith. (2013). *South Platte Decision Support System Alluvial Groundwater Model Report*(State of Colorado, Department of Natural Resources, Colorado Water Conservation Board). Retrieved April 18, 2018, from http://cdss.state.co.us/DSSDocuments/Pages/BasinReports.aspx

Colorado Division of Water Resources (CDWR). (1999). *State Engineer Guidelines For Lining Criteria For Gravel Pits* (pp. 1-3).

Colorado Division of Water Resources (CDWR). (2017). [SAINT VRAIN CREEK AT MOUTH NEAR PLATTEVILLE, CO (SVCPLACO)]. Raw data. Stream Gage

Colton, R. B. (1978). *Geologic map of the Boulder-Fort Collins-Greeley Area, Colorado*. Reston, VA: U.S. Geological Survey.

Doherty, J. (2001). Improved calculations for dewatered cells in MODFLOW. *Ground Water*, 39(6), 863-869. http://dx.doi.org/10.1111/j.1745-6584.2001.tb02474.x

Fetter, C. W. (2001). *Applied Hydrogeology* (4th ed.). Upper Saddle River, NJ: Prentice Hall. pp. 85

Gochis, D., Schumacher, R., Friedrich, K., Doesken, N., Kelsch, M., Sun, J., Ikeda, K., Lindsey, D., Wood, A., and Dolan, B. (2015). The great Colorado flood of September 2013. *American Meteorological Society Bulletin*, 96, 1461–1487. http://dx.doi.org/10.1175/BAMS-D-13-00241.1

Green, J. A., Pavlish, J. A., Merritt, R. G., & Leete, J. L. (2005). Hydraulic impacts of quarries and gravel pits. *Minnesota Department of Natural Resources, Division of Waters. Prepared for the Legislative Commission on Minnesota Resources*.

Harbaugh, A. W., Banta, E. R., Hill, M. C., & McDonald, M. G. (2000). MODFLOW-2000, The U. S. Geological Survey Modular Ground-Water Model-User Guide to Modularization Concepts and the Ground-Water Flow Process. *Open-file Report. U. S. Geological Survey*, (92), 134.

Jarrett, R. D. (1985). *Determination of roughness coefficients for streams in Colorado*. Lakewood, CO: U.S. Geological Survey.

Johnson, A. I. (1963). *Compilation of specific yield for various materials* (No. 63-59).

Lindsey, DA, WH Langer, LS Cummings, JF Shary (1998), Gravel Deposits of the South Platte River Valley North of Denver, US Geol Survey Open-File Report 98-148-A.

McDonald, M. G., & Harbaugh, A. W. (1988). *A modular three-dimensional finite-difference ground-water flow model*. Reston, Va.: U.S. Geological Survey.

Ober, J. A. (2017). *Mineral commodity summaries 2017*. US Geological Survey.

Prudic, D. E., Konikow, L. F., & Banta, E. R. (2004). *A new streamflow-routing (SFR1) package to simulate stream-aquifer interaction with MODFLOW-2000*. Carson City, NV: U.S. Dept. of the Interior, U.S. Geological Survey.

Rathburn, S.L., Bennett, G.L., Wohl, E.E., Briles, C., McElroy, B., and Sutfin, N. (2017). The fate of sediment, wood, and organic carbon eroded during an extreme flood, Colorado Front Range, USA. *Geology*, 45(6), 499-502. http://dx.doi.org/10.1130/G38935.1

Robson, S. G., Heiny, J. S., & Arnold, L. R. (2000a). Geohydrology of the shallow aquifers in the Boulder-Longmont area. *Colorado: US Geological Survey Hydrologic Investigations Atlas HA–746–D*, *5*.

Robson, S. G., Heiny, J. S., & Arnold, L. R. (2000b). Geohydrology of the shallow aquifers in the Fort Lupton-Gilcrest area. *Colorado: US Geological Survey Hydrologic Investigations Atlas HA-746-C*, *5*.

Robson, S. G., Van Slyke, G.D., & Graham, G. (1998). *Structure, outcrop, and subcrop of the bedrock aquifers along the western margin of the Denver Basin, Colorado*. U.S. Geological Survey Hydrologic Atlas 742.

Ronayne, M., Rach, G. (2018). *Influence of Lined Sand and Gravel Pits on Shallow Aquifers, Colorado Front Range*. Unpublished technical report.

Rosas, J., Lopez, O., Missimer, T.M., Coulibaly, K.M., Dehwah, A.H.A, Sesler, K., Lujan, L.R., Mantilla, D. (2014). Determination of Hydraulic Conductivity from Grain-Size Distribution for Different Depositional Environments. *Groundwater, 52*(3), 399-413. doi:10.1111/gwat.12078

Rumbaugh, J., & Rumbaugh, D. (n.d.). Groundwater Vistas (Version 6.74) [Computer software].

Schwochow, S. D., Shroba, R. R., & Wicklein, P. C. (1974). *Sand, gravel, and quarry aggregate resources, Colorado Front Range counties*. Denver, CO: Colorado Geological Survey, Dept. of Natural Resources, 1974.

Schneider, P. A. (1983). *Shallow ground water in the Boulder-Fort Collins-Greeley area, Front Range urban corridor, Colorado, 1975-77*. Lakewood, CO: U.S. Geological Survey.

SEO. (1999). *State Engineer Guidelines For Lining Criteria For Gravel Pits* (pp. 1-3). CO.
Smith, R. O., Schneider, P. A., & Petri, L. R. (1964). *Ground-water resources of the South Platte River Basin in western Adams and southwestern Weld Counties, Colorado*. Washington, D.C.: U.S. G.P.O.

Terracon. (2008). [Borehole Logs]. Unpublished raw data.

U.S. Geological Survey. 2015. National elevation data set (NED). Accessed 1 July 2017. https://nationalmap.gov/3DEP/

U.S. Geological Survey, 2017, National Water Information System data available on the World Wide Web (USGS Water Data for the Nation), accessed Jan. 10, 2017, at URL https://waterdata.usgs.gov/nwis/uv?site_no=06730525